J. Physiol. (1979), **288**, *pp.* 129–158
With 9 text-figures
Printed in Great Britain

EFFECTS OF EXTERNAL CALCIUM CONCENTRATION AND pH ON CHARGE MOVEMENT IN FROG SKELETAL MUSCLE

BY HAROLD H. SHLEVIN*

From the Department of Physiology, University of Rochester School of Medicine, Rochester, New York 14642, U.S.A.

(*Received 16 March 1978*)

SUMMARY

1. The effects of both external Ca^{2+} (1·8, 25, 50 and 100 mM) and external pH (pH 5·5, 7·15, and 9·0) on the voltage-dependence of charge movement in frog skeletal muscle were examined using the three intracellular micro-electrode voltage-clamp technique.

2. The two-state model of Schneider & Chandler (1973) was used to describe the voltage distribution of membrane charge. The parameters of this model are: Q_{max}, the maximum quantity of charge; $\bar{V}$, the potential of equal distribution of charge; and k, a constant relating to the steepness of the charge *vs.* voltage relationship.

3. In 1·8 mM external Ca^{2+}, alterations in external pH shifted the transition potential, $\bar{V}$, from a mean ± S.E. of mean of $-36{\cdot}5 \pm 0{\cdot}9$ mV at pH 7·15 to $-25{\cdot}8 \pm 1{\cdot}3$ mV at pH 5·5 and to $-42{\cdot}5 \pm 1{\cdot}8$ mV at pH 9·0. These shifts are consistent with surface charge theory. No significant changes in Q_{max} or k were observed over the range of pH 5·5–9·0.

4. A reasonable fit of surface charge theory to the shifts in $\bar{V}$ over the range pH 5·5–9·0 could be obtained with surface charge densities and binding constants: $\sigma_1 = -1e/165$ Å^2, $pK_1 = 3{\cdot}9$ and $\sigma_2 = -1e/400$ Å^2, $pK_2 = 8$.

5. However, at pH 7·15, both $\bar{V}$ and k changed with increasing external Ca^{2+} concentration. $\bar{V}$ shifted from $-34{\cdot}9 \pm 3{\cdot}7$ mV in 1·8 mM-Ca^{2+} to $-13{\cdot}8 \pm 5{\cdot}1$ mV, $-19{\cdot}3 \pm 3{\cdot}6$ mV and $3{\cdot}3 \pm 9{\cdot}3$ mV in 25, 50 and 100 mM-Ca^{2+} respectively. k increased from $8{\cdot}3 \pm 0{\cdot}6$ mV in 1·8 mM-Ca^{2+} to $15{\cdot}3 \pm 1{\cdot}4$ mV, $14{\cdot}6 \pm 1{\cdot}6$ mV and $20{\cdot}0 \pm 2{\cdot}9$ mV in 25, 50 and 100 mM-Ca^{2+}. Changes in k reflect decreases in the apparent charged particle valence from ~ 3 in 1·8 mM-Ca^{2+} to ~ 1·2 in 100 mM-Ca^{2+}. As the external Ca^{2+} concentration was raised, Q_{max} was at least as large as that measured in 1·8 mM-Ca^{2+}. The 43 % decrease in the apparent valence of the charged groups cannot be explained by simple surface charge theory and may reflect a specific interaction between external Ca^{2+} and the charged groups.

6. Shifts in $\bar{V}$ with alterations in external pH and Ca^{2+} concentration are consistent with the effects of these agents on the contraction threshold of muscle fibres. This observation lends further support to the hypothesis that the charge movement is involved in gating muscle contraction and that the charged particles respond to changes in the electric field across the muscle cell membrane.

* Present address: Mayo Graduate School, Mayo Clinic, Department of Pharmacology, Rochester, Minnesota 55901, U.S.A.

7. No difference was observed in the charge movement parameters of fibres from both room-temperature and cold-adapted frog tested at 2–5 °C in 1·8 mM-Ca^{2+} at pH 7·15.

INTRODUCTION

Under physiological conditions, contraction of skeletal muscle cells is initiated by depolarization of the membranes of the transverse tubular system, T-system (Huxley & Straub, 1958; Huxley & Taylor, 1958; Sandow, 1965; and Costantin, 1970). The T-system network provides the means whereby a change in surface potential can be rapidly transmitted to the interior of the fibre (Falk, 1968; Adrian, Chandler & Hodgkin, 1969; Adrian, Costantin & Peachey, 1969; Franzini-Armstrong, 1970, 1971, 1975). Subsequently, a potential change across the sarcoplasmic reticulum (SR) membrane (Bezanilla, Caputo & Horowicz, 1972; Bezanilla & Horowicz, 1975; Baylor & Oetliker, 1977*a*, *b*, *c*; Kovács & Schneider, 1977) is thought to mediate calcium release from the terminal cisternae of the SR (Winegrad, 1968). The contractile system is activated by the resultant increase in myoplasmic free Ca^{2+} concentration (Ebashi, Endo & Ohtsuki, 1969).

However, it is not yet clear how a potential change across the T-system membrane is communicated across the small gap separating the T-system and SR membranes. Recently it was suggested that the link involved the movement of charged particles free to move between different locations within the T-system membrane. This voltage-dependent charge movement in muscle is consistent with a molecular trigger mechanism for contractile activation (Schneider & Chandler, 1973; Adrian & Almers, 1976*a*, *b*; Chandler, Rakowski & Schneider, 1976*a*, *b*).

The present study was conducted to examine the effects of elevated external calcium ion concentrations and alterations of the external pH on the voltage dependence of intramembrane charge movement in frog skeletal muscle. If the shifts in the contraction threshold (Lüttgau, 1963; Costantin, 1968; Dörrscheidt-Käfer, 1976) reflect changes in the mechanism which gates the excitation-contraction coupling process in skeletal muscle fibres, one might expect to observe similar voltage-dependent shifts in the charge movement properties of muscle fibres under similar conditions.

The present study demonstrates for the first time (1) shifts in the transition voltage, $\bar{V}$, with alterations in external pH and (2) shifts in both $\bar{V}$ and k accompanying increases in the extracellular Ca^{2+} concentration. These shifts in the charge movement parameters are consistent in direction and generally consistent in magnitude with the reported effects of both pH and external Ca^{2+} concentration on the contraction threshold of frog muscle fibres. These observations lend further support to the hypothesis that the charge movement is involved in gating mechanical activation and that the charged particles respond to changes in the electric field across the muscle cell membrane. A brief report of this work has been presented (Shlevin, 1978).

METHODS

All experiments were performed at 2–5 °C on muscle fibres from the dorsal head of the semitendinosus muscle of North American *Rana pipiens*.

Frog maintenance

The physiological properties of muscle fibres isolated from cold-adapted and room temperature-adapted frogs differ (Dulhunty & Gage, 1973; Kovács & Schneider, 1977). Since these differences in the efficacy of excitation-contraction coupling might be reflected in the charge movement properties of the muscle fibres, one must clearly define the physiological state of adaptation of the frogs.

The frogs were maintained in one of two physiological states, room temperature-adapted (15–20 °C) or cold-adapted (2–6 °C) (Shlevin, 1977). Fibres from cold-adapted frogs were used exclusively in the experiments that were conducted from June 1976 to February 1977, which were designed to examine the effects of increased extracellular Ca^{2+} concentrations on muscle charge movement. In late February 1977, the muscle fibres of cold-adapted frogs became unsuitable for use in experiments. The membrane potential of fibres was unacceptably low in normal Ringer solution (i.e. -60 to -50 mV), and the fibres rapidly deteriorated further in solutions made hypertonic with sucrose.

To restore the experimental suitability of these muscles, frogs were adapted to a room-temperature environment and fed. Fibres from room-temperature adapted frogs had higher membrane potentials and greater longevity in hypertonic solutions. They were used exclusively in those experiments conducted from March 1977 to June 1977 which were designed to examine the effects of alterations in external pH on the voltage dependent properties of muscle charge movement.

Dissection

Muscle fibres from the dorsal head of the semitendinosus muscle were used to avoid slow fibres. Since the voltage-clamp technique (Adrian, Chandler & Hodgkin, 1966, 1970*a*) requires that the ends of individual fibres be clearly defined, further dissection was carried out under the dissecting microscope. The muscle was stretched from rest length into a rhombus by extending outward the medial aspect of each tendon. Superficial layers of fibres were then removed until a sheet of well separated individual fibres and small bundles of fibres at most one to two cell layers thick remained.

Voltage-clamp methodology

Individual muscle fibres were voltage-clamped at their pelvic end using the three intracellular micro-electrode voltage-clamp technique developed by Adrian *et al.* (1966, 1970*a*). The methodology used to measure the charge that is placed across the fibre capacitance during a voltage step imposed at the site of impalement of the V_2 micro-electrode was developed by Schneider & Chandler (1976). The methodology for measuring capacitance using the three intracellular micro-electrode voltage-clamp technique is independent of whether the potential at distance $x = l$ or that at distance $x = 2l$ is used as the controlled voltage, provided that both V_1 and V_2 reach steady levels by the end of the command pulse (Fig. 1*A*, *B*).

Voltage-recording micro-electrodes were directly filled by boiling in 3 M-KCl under reduced pressure. Current-passing micro-electrodes were filled by diffusion (Tasaki, Polley & Orrego, 1954) with approximately 2·8 M-potassium citrate. The resistance of all voltage-monitoring micro-electrodes was carefully matched (*q.v.* Schneider & Chandler, 1976); their resistance ranged from 8 to 11 MΩ with tip potentials < 6 mV as measured in normal Ringer solution. The resistance of current-passing micro-electrodes ranged from 8 to 10 MΩ. Current-passing micro-electrodes were carefully shielded by a grounded metal tube and painted (Valdiosera, Clausen & Eisenberg, 1974) with conductive lacquer and then insulated to within < 1 mm of the visible end of their tips.

Cable parameters

Applying the theory developed by Adrian *et al.* (1970*a*), i_m, the current density at distance $x = l$ from the end of the fibre is approximated as

$$i_m(t) = \frac{2}{3l^2 r_i} \Delta V(t), \quad (1)$$

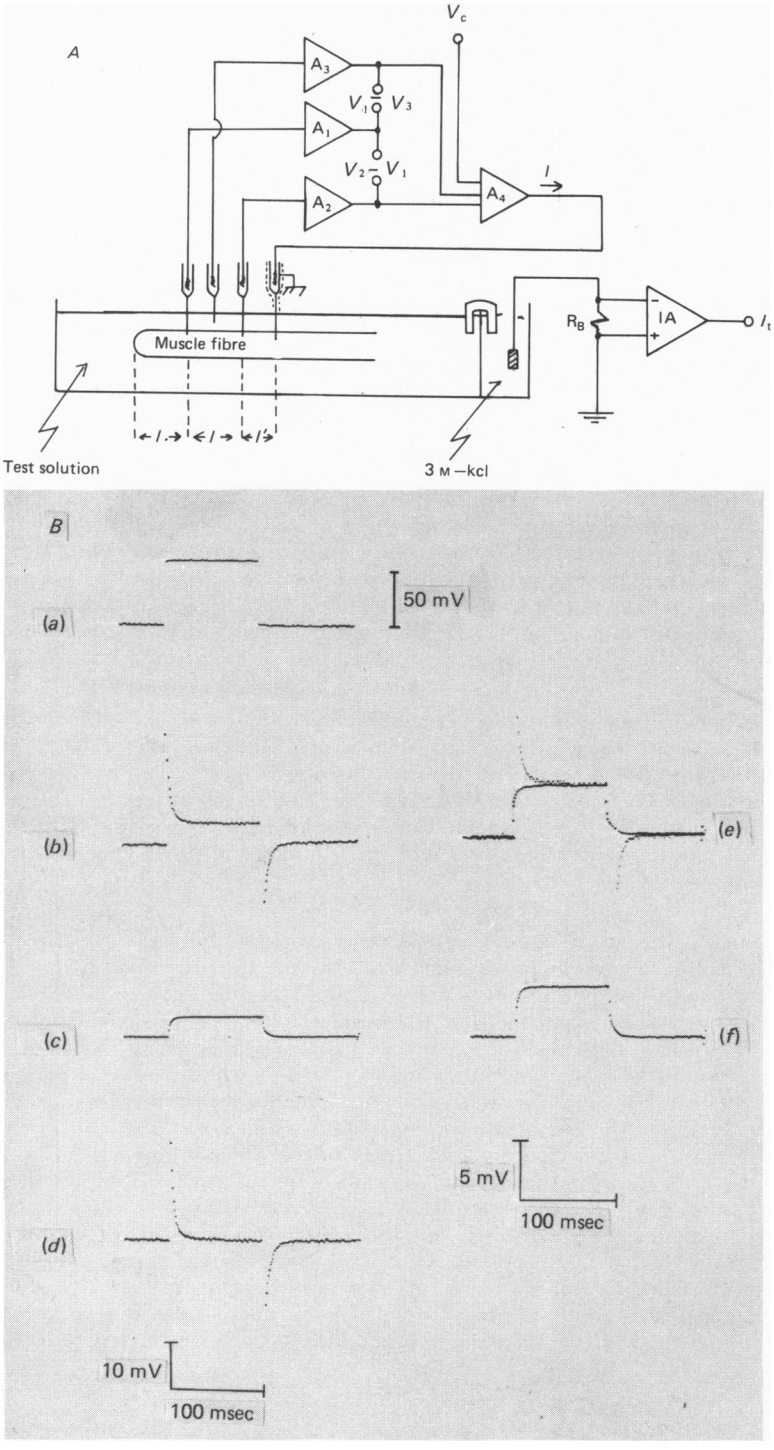

Fig. 1. For legend see facing page.

where r_i is the internal longitudinal resistance per unit length of fibre, l is the distance from the end of the cell to the V_1 micro-electrode, and $\Delta V(t)$ is the difference in potential recorded by the micro-electrodes positioned at distance $x = l$ and $x = 2l$ from the end of the cell. The fibre space constant, λ, and the internal resistivity of the myoplasm, r_i, were determined from steady-state displacements of V_1, ΔV, and I_o; the apparent radius, a, of the assumed cylindrical fibre was calculated from values of r_i and R_i (Adrian *et al.* 1970*a*). R_i, the specific resistivity of the myoplasm, was calculated as a function of temperature and tonicity from the data of Hodgkin & Nakajima (1972).

The effective capacity, $C_{eff}/V_1(\infty)$, is approximated using the time integral of capacitative current per unit fibre length as:

$$C_{eff} \approx \frac{2}{3l^2 r_i V_1(\infty)} \int_0^\infty \left[\Delta V(t) - V_1(t)\frac{\Delta V(\infty)}{V_1(\infty)}\right] dt \qquad (2)$$

(Schneider & Chandler, 1976).

Data acquisition

The analogue signals $(V_2 - V_3)$ and ΔV were digitized using a voltage-to-frequency conversion technique and digitally tape recorded using a custom-designed data acquisition system (Shlevin, 1976). The $(V_2 - V_3)$ and ΔV signals could not be digitized simultaneously as only a single V/F converter was available. Generally, for any sequence of test pulses, the ΔV signals were digitized and tape recorded first. Immediately thereafter, the same sequence of test pulses was repeated

---

Fig. 1. *A*, schematic diagram of the voltage-clamp apparatus. Three micro-electrodes were inserted into the pelvic end of a muscle fibre. They were positioned at distance l, $2l$, and $(2l+l')$ from the end of a fibre and were used to record potentials V_1, V_2, and to inject current, I, respectively. A fourth micro-electrode, positioned just outside the fibre at distance $\frac{3}{2}l$ from the end of the fibre was used to record potential V_3. V_3 was used to correct for potential changes in the bath. Potentials V_1, V_2, and V_3 were monitored using unity gain, high input impedance voltage followers A_1, A_2, and A_3, respectively. A negative feedback circuit, A_4, passed current as necessary to minimize the difference between the potential being clamped, viz. $(V_2 - V_3)$, and the commanded potential, V_c. The experimental bath was grounded through a 1 kΩ resistor, R_B. The total current, I_o, was monitored by measuring the IR drop across R_B using dual FET followers (not known) as inputs to an instrumentation amplifier, IA. The bath was electrically coupled to the current-measuring circuit by a 2% (wt./vol.) agar bridge which was immersed in a 3 M-KCl pool fitted with a Ag/AgCl pellet electrode. Since the bath was close to earth potential, V_3 was also close to earth potential except during the 'make' and 'break' of the voltage clamp step.

B, method of area analysis. Digitized data records obtained from a voltage-clamped muscle fibre are shown. The three intracellular micro-electrode voltage-clamped technique (Adrian *et al.* 1970*a*) was used to apply a step change in potential at the site of impalement of the V_2 micro-electrode. Records *a*–*f* represent: *a*, $(V_2 - V_3)$, the potential at the clamped point; *b*, ΔV, the potential difference $(V_2 - V_1)$ where V_2 and V_1 are the potentials recorded at distances $2l$ and l from the end of the fibre (*q.v.* eqn. (1)); *c*, $\bar{V}_1$, the computer calculated and scaled V_1 record. The scaled V_1 record, proportional to the ionic current component in ΔV, was computed by scaling the calculated V_1 record by the factor, $\Delta V(\infty)/V_1(\infty)$; *d*, the difference between the ΔV and $\bar{V}_1$ records; this record is proportional to capacitative current. The area under the transient portions of record *d* is proportional to the charge carried by the capacitative currents. The 'on' area was evaluated from the time corresponding to the 'on' of the test pulse to the time when both the V_1 and the ΔV records had reached their steady levels during the pulse; the 'off' area was similarly evaluated starting from the end of the test pulse; *e*, the $\bar{V}_1$ record and ΔV records redrawn at higher gain to illustrate that the $\bar{V}_1$ record scales to match the steady level of the ΔV record; and *f*, $\bar{V}_1$ at higher gain for comparison with *e*. See Schneider & Chandler (1976) for further description. Fibre reference F54, three times hypertonic solution B, temperature 5 °C, l = 267 μm, l' = 44 μm; 1 mV on ΔV corresponds to 0·084 μA/cm (eqn. (1)). $(V_2 - V_3)$ = 50·13 mV.

while the $(V_2 - V_3)$ signal was digitized and tape recorded. Since $(V_2 - V_3)$was the controlled voltage, it tended to remain constant during the experiment and changed less than 1 %. Successive test pulses, superimposed on the holding potential, caused $V_2(\infty)$ to traverse a voltage range of usually -150 to $+50$ mV, in increments of nominally 10 mV.

During each sequence of test pulses, the steady-state total current and membrane potential at V_1 during smaller test pulses of ± 20 mV from the holding potential were used to calculate λ and r_i. For larger test pulses, the photographed $(V_1 - V_3)$ and $(V_2 - V_3)$ signals were used to check the ability of the current passing micro-electrode to maintain the commanded potential constant. They also allowed the actual $(V_1 - V_3)$ signal to be compared with that V_1 signal calculated during analysis of the data by the computer. Slow changes of ΔV or of I_0 were followed on a single channel strip-chart recorder.

Calculation of the extra charge

Using values of total charge determined by area analysis (Fig. 1*B*) the extra charge was then evaluated. The procedure was to: (1) estimate linear fibre capacitance by fitting a linear least-squares line through the origin and through the 'on' and 'off' values of total charge at V_1 voltages negative to the usual holding potential of -100 to -80 mV; the correlation coefficient of the least-squares line was always greater than 0·96, (2) calculate and then normalize the extra charge to the linear capacitance of the fibre, the extra charge being calculated by subtracting the charge predicted for the linear capacitance (using linear extrapolation) at a given V_1 voltage from the total quantity of charge actually measured. By referring all current measurements to c_m, the factor $2/(3l^2r_i)$ cancels out (eqn. (2)) and thereby cancels the effects of small changes in r_i (Schneider & Chandler, 1976); (3) evaluate the relationship between charge and voltage, the normalized extra charge, viz. $nC/\mu F$, was then plotted as a function of the steady, calculated V_1 voltage to produce a charge *vs.* voltage, Q–V, curve which was then fitted, in a non-linear least-squares manner, to a two-state Boltzmann distribution (Schneider & Chandler, 1973, 1976):

$$Q(V) = \frac{Q_{max}}{1 + \exp[-(V - \bar{V})/k]} \tag{3}$$

The parameters of this model are: Q_{max}, the maximum quantity of charge; $\bar{V}$, the potential of equal distribution of charge; and k a constant related to the steepness of the Q–V relationship. k is given by $|RT/(AzF)|$ where A is a constant independent of voltage; R, T, and F have their usual meaning, and z is the apparent valence of the particle. Assuming that the moving charges sense the entire membrane field, viz. $A = 1$, then the effective valence, $z = (RT/F)/k$.

In fitting the Q–V curves, the arithmetic mean of the extra charge calculated for both the pulse 'on' and pulse 'off' periods was used when a ΔV record had not been corrected. However, when a ΔV record was corrected for an outward conductance during the pulse, the extra charge calculated for only the pulse 'on' period was used in fitting the Q–V curve to assure that all voltages were equally weighted by the curve-fitting programme. A correction procedure was only used on the ΔV records recorded from fibres in high Ca^{2+} solutions that exhibited delayed rectification.

Solutions

The composition of the experimental solutions is given in Table 1.

Since overt movement was blocked by sucrose hypertonicity in the test solutions, the following criteria were used to indicate the viability of individual fibres during an experiment: (1) the fibre viewed through the dissecting microscope had to appear internally clear and homogeneous, (2) the membrane potential upon initial penetration had to be greater, viz. more negative, than -80 mV. In addition, the membrane potential must have remained greater than -75 to -80 mV after all three micro-electrodes had been positioned in the cell, (3) during the experiment, the final criterion was a low and stable holding current.

TABLE 1. Composition of experimental solutions

Experiments designed to examine the effects of elevated extracellular Ca^{2+} concentration were performed at pH 7·15 at 2 to 5 °C in solutions buffered by 1 mM-Tris-acid maleate. Solution pH was adjusted at room temperature to be 7·15 at the experimental temperature assuming a buffer temperature coefficient of 0·03 pH units per °C (Sigma Chemical Co., 1972). The wider range buffer system, 2 mM-N-acetylglycine and 2 mM-Tris-acid maleate (Hutter & Warner, 1967) was used; the buffering capacity was measured in solutions F–J and found to be relatively constant over the range pH 4–9·8. To block movement, experimental solutions B–J were freshly made three times hypertonic with sucrose (Hodgkin & Horowicz, 1957). Sucrose addition was calculated according to the formulation by Dydyńska & Wilkie (1963), and was adjusted, allowing for the osmotic coefficient and activity (Robinson & Stokes, 1970; Weast & Selby, 1962) of other solutes, to maintain a constant tonicity in all solutions

		Composition [mM]							
Ref.		Ca^{2+}	K^+	Na^+	Rb^+	TEA^+	Cl^-	$C_6H_9O_6^-$	SO_4^{2-}
A	Normal Ringer	1·8	2·5	115·0	—	—	121·1	—	—
B	1·8 Ca-TEA.Cl	1·8	—	—	5·0	117·5	126·1	—	—
C	25 Ca-TEA.Cl	25·0	—	—	5·0	117·5	172·5	—	—
D	50 Ca-TEA.Cl	50·0	—	—	5·0	117·5	222·5	—	—
E	100 Ca-TEA.Cl	100·0	—	—	5·0	117·5	322·5	—	—
F	1·8 Ca-TEA.G	1·8	—	—	5·0	117·5	—	126·1	—
G	25 Ca-TEA.G	25·0	—	—	5·0	117·5	—	172·5	—
H	50 Ca-TEA.G	50·0	—	—	5·0	117·5	—	222·5	—
I	100 Ca-TEA.G	100·0	—	—	5·0	117·5	—	322·5	—
J	1·8 Ca-TEA.S	1·0*	—	—	5·0	117·5	—	—	62·3

* Made using 8 mM-$CaSO_4$. The concentration of ionized calcium is approximately 1 mM if the dissociation constant for $CaSO_4$ is $5·3 \times 10^{-3}$ mole/l. (Hodgkin & Horowicz, 1959). Solutions B–J also contained 1 mM-4-aminopyridine and 10^{-6} g TTX/ml. G = glucuronate, S = sulphate.

RESULTS

Effects of external pH on charge movement

Changes in the voltage-dependent properties of muscle charge movement were measured at pH 7·15, 5·5 and 9·0. Experiments were restricted to this pH range because fibres bathed in three times hypertonic solutions at pH lower than 5·0 or at pH greater than 10 rapidly deteriorated.

To reduce fibre-to-fibre variability and to allow each fibre to serve as its own control, the experiments, whenever possible, were performed on the same fibre in solutions of different pH. The three micro-electrodes were left in the cell during the solution change as it was usually not possible to successively re-impale the same cell at the same loci without inducing substantial damage. Due to the sensitivity of the cell membrane, this procedure was successful in somewhat less than 50% of the attempts (nineteen fibres from nine muscles). No correction was applied to the experimental data and no signal averaging was used in analysing the results of the pH experiments. Thirteen fibres from five muscles were not analysed due to the appearance of a slow decrease in outward current for depolarizing pulses to beyond approximately -40 mV. Since the latter ΔV records were not flat at the end of

the 100 msec voltage pulses, the steady-state properties of membrane charge movement could not be determined in these fibres. The kinetic characteristics of this slow current which resembles the slow inward calcium current (Stanfield, 1977) have not been described. Therefore, no theoretical foundation for correcting this data exists. This observation is discussed in a later section.

To avoid pH-induced changes in the voltage- and time-dependent properties of the chloride conductance (Hutter & Warner, 1972; Warner, 1972), all pH experiments were performed in chloride-free solutions F or J (Table 1). An equilibration time of 1·6–1·8 hr was allowed to wash out the internal chloride before any measurements were performed. The excitability of the preparation was checked by external stimulation and the bathing solution was subsequently made three times hypertonic with sucrose.

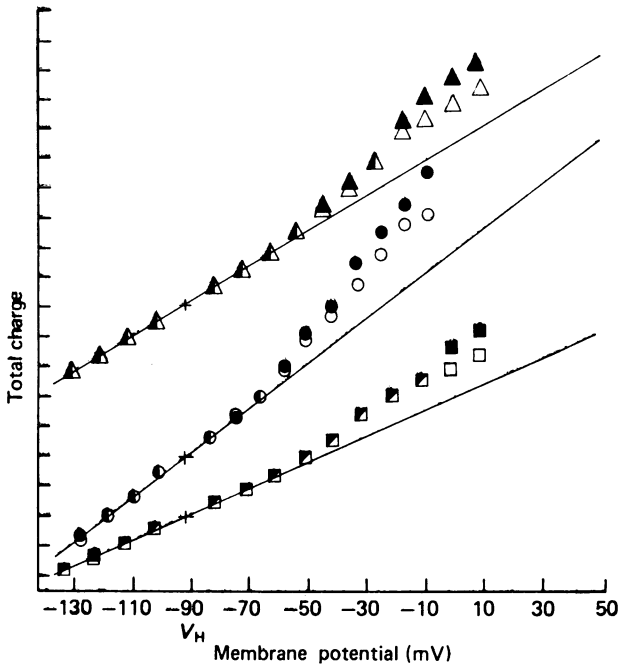

Fig. 2. Relationship between total charge and membrane potential at pH 5·5 and pH 7·15. The absolute value of total charge in arbitrary units determined for the pulse 'on' period, (open symbols) and for the pulse 'off' period, (filled symbols) is plotted as a function of the steady, calculated V_1 voltage (mV). Each curve is vertically displaced for purposes of clarity. The continuous lines represent the best linear least-squares fit to the data points negative to the holding potential, V_H, − 92 mV. The slope of this line is proportional to the linear fibre capacitance. The first measurements were performed at pH 5·5 (△, ▲); the bathing solution was then exchanged for like solution buffered to pH 7·15 (○, ●); finally, the bathing solution was returned again to pH 5·5 (□, ■). Solution F (*q.v.* Table 1) made three times hypertonic with sucrose. Fibre F81. Temperature 5 °C. Electrodes remained in the cell during this sequence of solution changes; the holding current was low and stable throughout.

Charge measurements at pH 5·5 and pH 7·15

Fig. 2 illustrates the results of the capacitance analysis from a fibre in solution F made three times hypertonic with sucrose. The sequence of solution changes for this particular fibre were: (1) pH 5·5; (2) pH 7·15; and (3) again, pH 5·5. The electrodes remained within the cell during this sequence of solution changes. Even for depolarizations to as positive as +9 mV, the ΔV records were decidedly flat by the end of the pulse.

TABLE 2. Effects of pH on charge movement. The curve fit parameters, viz. Q_{max} ($nC/\mu F$), $\bar{V}$ (mV), and k (mV) as well as an error parameter for the fit, Error (mV^2), the linear fibre capacitance (L.f.c.) and the calculated λ (cm), and r_1 (MΩ/cm) head columns IV–X of this Table. The solution pH, fibre reference and test solution (Table 1) are indicated in columns I–III. The sequence of solution changes performed on each fibre is denoted by the numeral in column III which follows the solution reference. The grand mean ± S.E. of mean for each parameter is shown after each pH sequence. When an individual fibre was tested at the same pH twice, the averaged value of that parameter for the two runs at the same pH was used in calculating the over-all mean. This procedure assured that each fibre was equally weighted in calculating the grand mean

I	II	III	IV	V	VI	VII	VIII	IX	X
pH	Fibre	Solution/ sequence	Q_{max} ($nC/\mu F$)	$\bar{V}$ (mV)	k (mV)	Error (mV^2)	L.f.c.	λ (cm)	r_1 (MΩ/cm)
5·5	80	F/2	37·2	−23·8	12·8	0·51	2·7	0·098	10·92
	81	F/1	38·9	−25·4	11·5	0·80	2·9	0·135	13·99
		F/3	31·3	−29·8	9·8	0·76	2·2	0·095	13·48
	89	J/1	35·4	−27·2	10·8	0·82	1·5	0·172	10·17
		J/2	38·0	−30·0	10·4	1·0	1·5	0·168	10·48
	96	J/2	36·7	−23·2	12·0	1·0	1·1	0·189	7·83
Mean ± S.E. of mean			36·4 ± 0·5	−25·8 ± 1·3	11·5 ± 0·5	—	2·0 ± 0·4	0·143 ± 0·02	10·7 ± 1·21
7·15	80	F/1	34·5	−35·1	9·2	0·99	2·4	0·091	12·36
	81	F/2	36·3	−37·7	10·8	1·12	3·7	0·078	11·63
	88	J/1	21·6	−38·2	8·6	0·14	2·3	0·224	8·3
	95	F/1	30·2	−35·6	12·0	1·12	2·2	0·139	15·41
		F/3	34·1	−34·3	12·0	1·35	2·0	0·135	15·3
Mean ± S.E. of mean			31·1 ± 3·3	−36·5 ± 0·9	10·2 ± 0·8	—	2·6 ± 0·4	0·133 ± 0·03	11·91 ± 1·4
9·0	94	F/1	24·2	−42·6	10·7	0·96	4·8	0·101	9·93
	95	F/2	37·4	−45·6	10·7	1·26	1·3	0·091	14·62
	96	J/1	42·1	−39·4	13·6	0·87	1·6	0·113	13·29
Mean ± S.E. of mean			34·6 ± 5·4	−42·5 ± 1·8	11·7 ± 1·0	—	2·6 ± 1·1	0·102 ± 0·01	12·6 ± 1·4

The linear fibre capacitance was estimated by fitting a linear least-squares line through those data points negative to the holding potential, $V_H = -92$ mV. The slope of the resultant line is proportional to the linear capacitance. For all fibres measured, the mean change in linear capacitance for changes in external pH were not significant (*q.v.* Table 2).

For each run, the extra charge was then calculated and normalized to the linear

capacitance. The result of this procedure for the same fibre of Fig. 2 is shown in Fig. 3*A*. The continuous lines in Fig. 3*A* represent the best non-linear least-squares fit of the data to eqn. (3). The data and theoretical best-fit of eqn. (3) agree very well over a voltage range negative to −10 mV. For voltages greater than −10 mV, the extra charge calculated for the pulse 'on' and 'off' periods differ.

Fig. 3*B* illustrates the correspondence of Q_{on} and Q_{off} for the three runs on the

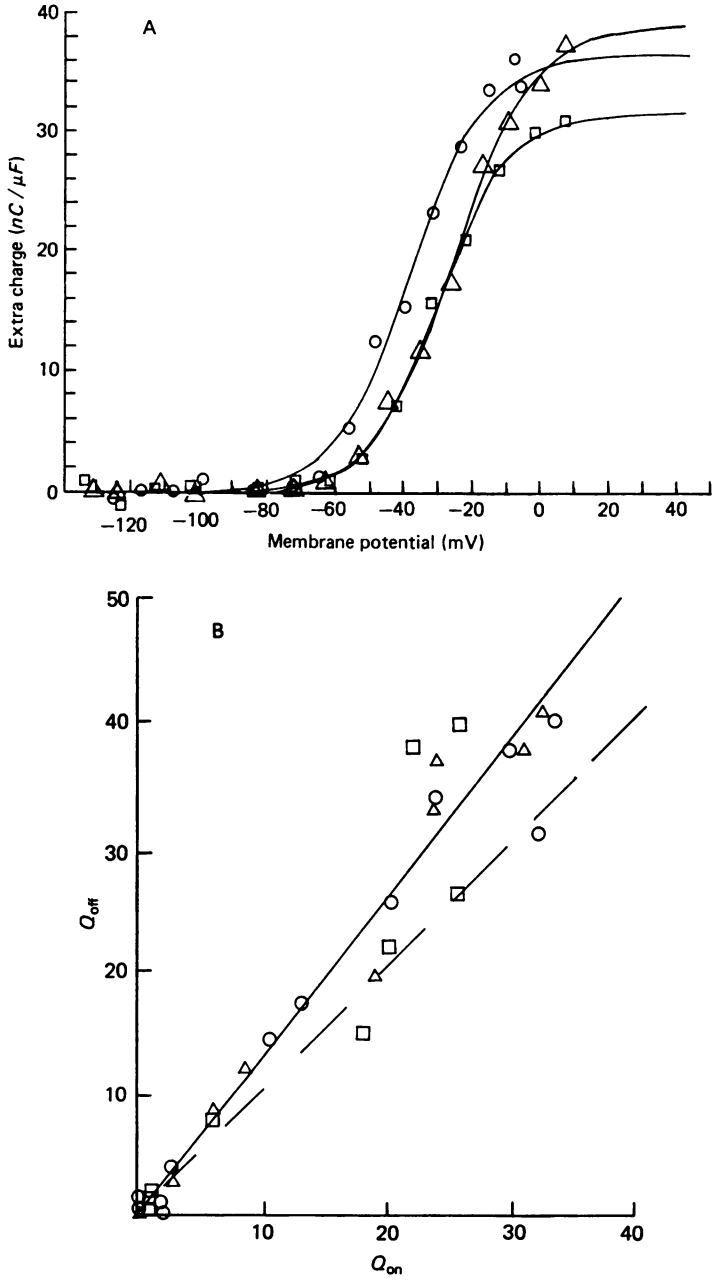

Fig. 3. For legend see facing page.

same fibre of Fig. 2. All values of Q_{on} and Q_{off} from this fibre at voltages greater than the holding potential were analysed by linear regression analysis of the form $Q_{off} = mQ_{on}+b$. The dashed line represents $Q_{off} = -Q_{on}$; the continuous line represents the regression line.

These results in Fig. 3*A* demonstrate that for a change in pH from 5·5 to 7·15, the transition voltage, $\bar{V}$, shifts along the voltage axis by 12 mV in a hyperpolarizing direction from $-25{\cdot}4$ to $-37{\cdot}7$ mV, respectively. On return to identical solution at pH 5·5, the parameter $\bar{V}$ returns to the control values, $-29{\cdot}8$ mV. There was essentially no significant change in Q_{max} or k over this pH range.

Summary of pH effects

The charge movement parameters derived from the curve-fitting procedure for six fibres in solutions of various pH are tabulated in Table 2. The results of the pH experiments demonstrate a shift in the $\bar{V}$ parameter along the voltage axis from means ± S.E. of mean of $-36{\cdot}5 \pm 0{\cdot}9$ mV at pH 7·15 in a depolarizing direction to $-25{\cdot}8 \pm 1{\cdot}3$ mV ($\alpha < 0{\cdot}001$) at pH 5·5, and in a hyperpolarizing direction to $-42{\cdot}5 \pm 1{\cdot}8$ mV ($0{\cdot}02 < \alpha < 0{\cdot}05$) at pH 9·0. These changes are statistically significant. The k parameter, viz. $\approx$ 11 mV, is unchanged ($0{\cdot}2 < \alpha < 0{\cdot}3$) by altering the external pH over the range studied. Small changes in the parameter Q_{max} are probably not significant ($0{\cdot}2 < \alpha < 0{\cdot}5$). The linear fibre capacitance is not significantly altered by changing external pH in this fashion ($0{\cdot}2 < \alpha < 0{\cdot}5$), nor are the cable parameter λ and r_i ($\alpha < 0{\cdot}5$ and $0{\cdot}4 < \alpha < 0{\cdot}5$, respectively).

Fig. 3. *A*, steady-state charge normalized to fibre capacitance at pH 5·5 and pH 7·15. Charge displacements were obtained by averaging the 'extra charge' determined for the pulse 'on' and pulse 'off' periods of fibre F81. The theoretical curves were drawn according to eqn. (3) which was fitted to the averaged data points at voltages more positive than the holding potential. The first run was performed at pH 5·5 (△). Then the bathing solution was exchanged for like solution buffered to pH 7·15 (○). Finally, the bathing solution was returned to pH 5·5 (□). The best fit parameters for each run are shown below. Solution F made three times hypertonic with sucrose. Holding potential, -92 mV. Same fibre as shown in Fig. 2, fibre F81. The parameter, Error, represents the sum squared deviation between the observed data and the calculated best-fit.

Best fit parameters for fibre F81

Run	pH	Q_{max} (nC/μF)	$\bar{V}$ (mV)	k (mV)	Error (mV²)
1 (△)	5·5	38·9	$-25{\cdot}4$	11·5	0·80
2 (○)	7·15	36·3	$-37{\cdot}7$	10·8	1·12
3 (□)	5·5	31·3	$-29{\cdot}8$	9·8	0·76

B, Q_{on} and Q_{off} at different test potentials. 'Extra charge' (nC/μF) calculated for the pulse 'on' period is plotted against that calculated for the pulse 'off' period. 'Extra charge' values determined on fibre F81 for voltages greater than the holding potential were analysed by linear regression analysis of the form: $Q_{off} = mQ_{on}+b$. The best fit parameter were slope, $m = 1{\cdot}3$; intercept, $b = +0{\cdot}06$; correlation coefficient, $r^2 = 0{\cdot}96$. This regression line is indicated by the continuous line. The dashed line drawn at an angle of 45° represents $Q_{off} = -Q_{on}$. Symbols: △, pH 5·5, run 1; ○, pH 7·15, run 2; and □, pH 5·5, run 3. Same fibre as Figs. 2 and 3*A*.

Slow decreases in outward current

A slowly decreasing outward current was observed in a total of twenty-five fibres from thirteen muscles bathed in chloride-free solutions (solutions F–J, Table 1). The effect was never observed by this investigator in solutions containing chloride as the principle anion (Solutions B–E, Table 1).

Stanfield (1977) using a two-electrode voltage-clamp technique has recently and very briefly described net inward and 'inward-going' calcium currents in frog muscle fibres. The currents develop very slowly, reaching a maximum in about 500 msec at +4 mV at 18–20 °C in solutions containing sulphate as the principle anion. Stanfield (1977) did not describe the kinetic behaviour of this current.

The experimental solutions F and J (*q.v.* Table 1), used in the experiments

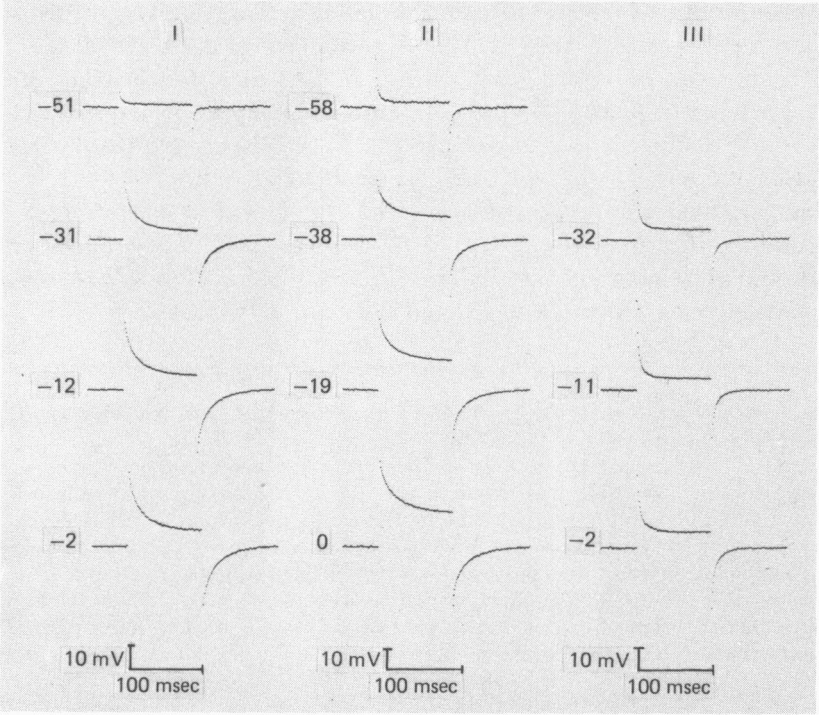

Fig. 4. ΔV records showing slow decreases in outward current during depolarizing voltage pulses. The ΔV records in column I are from fibre F84 (pH 7·15, solution F, 3 °C). A small and very slowly decreasing outward current is seen at −31 mV. This effect is somewhat more obvious at −12 and −2 mV. In column II, ΔV records from fibre F85 (pH 7·15, solution J, 2 °C) which illustrate the same phenomenon, are shown. In column III, ΔV records from fibre F81 (pH 7·15, solution F, 5 °C) at approximately the same potentials as the records in column I and II are shown. In column III, under similar conditions to column I and column II, the ΔV records are flat by the end of pulses of approximately the same amplitude and duration. Note that ΔV records for smaller depolarizing pulses of −51 and −58 mV of fibre F84 and fibre F85 are flat. Cable analysis of fibre F84 gave: $\lambda = 0{\cdot}095$ cm, $r_i = 14{\cdot}10$ MΩ/cm; $a = 29{\cdot}2$ μm, for $l = 267$ μm, $l' = 71{\cdot}2$ μm. Cable analysis of fibre F85 gave $\lambda = 0{\cdot}112$ μm, $r_i = 10{\cdot}89$ MΩ/cm, $a = 33{\cdot}8$ μm, for $l = 240{\cdot}3$ μm, $l' = 62{\cdot}3$ μm. In both experiments, the holding potential was −92 mV. Cable analysis of fibre F81 gave $\lambda = 0{\cdot}078$ cm, $r_i = 11{\cdot}63$ MΩ/cm.

reported here were similar in composition to those used by Stanfield (1977). Under these conditions, a slow decrease in outward current that appeared at approximately -40 mV was observed. An example is shown in Fig. 4 from two fibres: fibre F84 (column I) at pH 7·15 in Solution F at 3 °C, and fibre F85 (column II) at pH 7·15 in Solution J at 2 °C. In both fibres F84 and F85 no slow conductance changes were evident for hyperpolarizing pulses to -135 mV. In fibres F84 and F85 no slow conductance changes were evident for depolarizing pulses up to -51 mV and -58 mV, respectively. For comparison, ΔV records from a third fibre F81 (column III) which did not show any evidence of a slow decrease in outward current are shown.

An attempt was made to fit such ΔV records from four fibres to an exponential with a long time constant, and then to subtract off the 'inward-going' component during the pulse 'on' period. These corrected records were then analysed to measure the charge movement as described earlier. The parameter Q_{max} was consistently low, viz. 10–20 nC/μF; the uncorrected 'off' areas for voltages as small as -40 mV were consistently larger than the 'on' areas by at least 35 %. Attempts to exponentially fit and to correct the 'off' portion of a record were unsuccessful. Since the kinetics of such inward currents have not been described and since the results of the charge analysis of exponentially corrected records were inconsistent with previously reported results under control conditions and also under experimental conditions where there was no change in conductance during the pulse, no further attempt was made to analyse these ΔV records.

Effects of external Ca^{2+} concentration on ΔV

Although the composition of the experimental solutions was designed to minimize time- and voltage-dependent changes in membrane conductances (Schneider & Chandler, 1973, 1976), the block of such changes was never complete. Small outwardly directed changes in membrane current during large depolarizing voltage steps, i.e., above -30 to -20 mV, were apparent in all solutions with greater than 1·8 mM-Ca^{2+}. As the external Ca^{2+} concentration was elevated, progressively larger changes in membrane conductance occurred during the larger depolarizing voltage steps.

Fig. 5 illustrates the effects of increasing the extracellular Ca^{2+} concentration on ΔV records at pH 7·15. Traces *a* and *b* are from fibre F54 in 50 mM-Ca^{2+}, solution D, made three times hypertonic with sucrose. There is evidence of a very small conductance change associated with the depolarizing pulses to -3 and $+15$ mV. This is more evident in records *c–g*, from the same fibre, F54, in 100 mM-Ca^{2+}, solution E made three times hypertonic with sucrose. As the voltage pulse made the membrane potential more positive, progressively larger outward currents became evident. These currents turned on progressively more rapidly as the membrane was further depolarized. In fibre F54, no outward conductance changes were evident for $V \leqslant 0$ mV in 1·8 mM-Ca^{2+}, solution B.

A correction must be made for these changes in membrane conductance which prevent a clear resolution of the steady-state charge movement at large voltages in solutions with elevated external Ca^{2+} concentrations.

Correction procedure

The correction procedure that was adopted is similar to that used by Chandler *et al.* (1976*b*) who showed that, in the absence of any blocker of the delayed outward potassium channel, it is still possible to resolve mathematically the current

due to the charge movement from the outward current carried by K ions over a limited potential range where the larger outward potassium current did not swamp the charge transient. They fitted the ΔV points during the voltage pulse to the

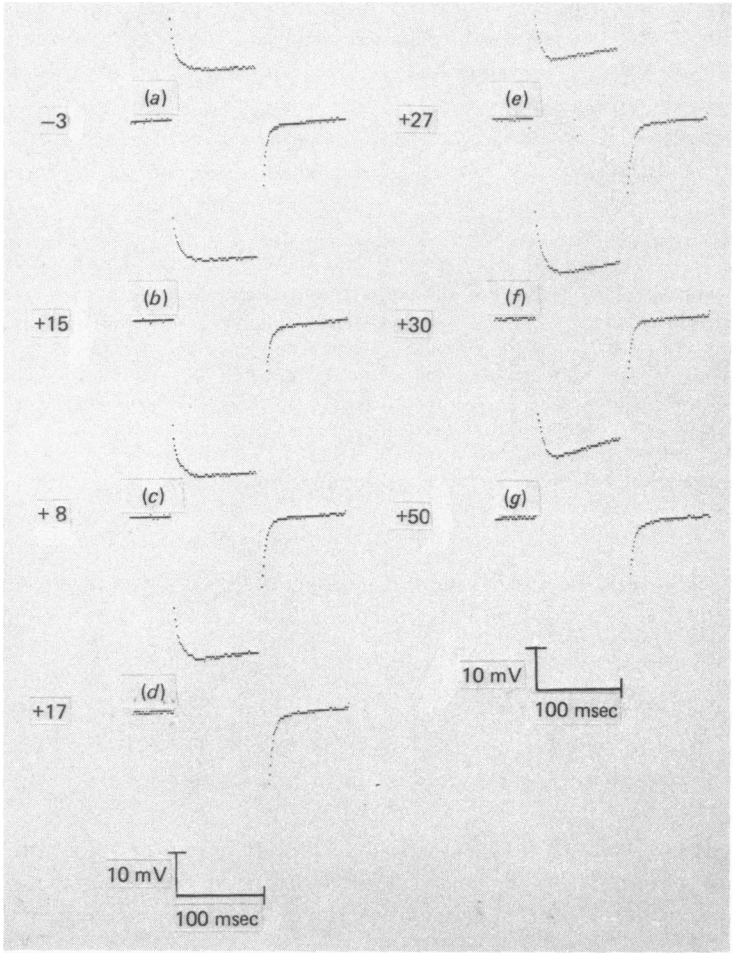

Fig. 5. Effect of external Ca^{2+} on ΔV records. These raw ΔV records are from fibre F54 at pH 7·15 in 50 mM and 100 mM-Ca^{2+}, three times hypertonic solutions D and E, respectively. Traces *a* and *b* were recorded in 50 mM-Ca^{2+}; traces *c–g* were recorded in 100 mM-Ca^{2+}. The voltage to the left of each ΔV record is the steady, calculated V_1 voltage for the corresponding corrected ΔV record. Traces *a* and *b* show a very small outward current component. The effect of Ca^{2+} on ΔV records is more pronounced in traces *c–g*, where the magnitude of the current and its rate of turn on increase with depolarization.

general equation: $\Delta V = \Delta V_K + \Delta V_Q$. ΔV_K represents the potassium current component and ΔV_Q represents the charge movement component:

$$\Delta V_K = \Delta V_K(\infty)\,[1-\exp(-t/\tau_n)]^4 \quad \text{and}$$
$$\Delta V_Q = \Delta V_Q(\phi)\,[\exp(-t/\tau_Q)].$$

In the experiments of Chandler *et al.* (1976*b*), the membrane potential $(V_1 - V_3)$ at $x = l$ was clamped; in contrast, in the experiments reported here, the membrane

potential ($V_2 - V_3$) at $x = 2l$ was clamped. In these experiments, linear components were not subtracted before curve fitting and therefore it was necessary to modify the equation for ΔV (Chandler *et al.* 1976*b*) by the addition of a constant, W, which determined the steady conductance during the pulse.

In the experiments reported here, 117·5 mM-tetraethylammonium (TEA) was always present in the bathing solution, and therefore the outward potassium currents, although present, were smaller than those observed by Chandler *et al.* (1976*b*). The potassium current, with rare exceptions at $> +20$ mV, was never large enough to swamp the charge transient. Therefore, it was usually possible to correct the ΔV records for the outward potassium current component.

The correction procedure is illustrated in Fig. 6*A*. The original data from Fig. 6*A* and its best fit are redrawn at higher gain in Fig. 6*B*. In all cases, the correction procedure was applied to the 'on' portion of the raw ΔV record. The corrected ΔV record was then re-analysed to calculate the V_1 record which would have occurred had there been no outward potassium current. The 'off' portion of the record was not corrected because it was contaminated by an inward potassium current tail that could not be resolved from the charge transient.

One of the original criteria for measurement of the intramembrane charge movement was that it must not represent an ionic current (Armstrong & Bezanilla, 1973*a*, *b*, 1974; Bezanilla & Armstrong, 1975; Schneider & Chandler, 1973; Chandler *et al.* 1976*a*, *b*; Adrian & Almers, 1976*b*). This criterion was validated by observing an equality of charge moved during the 'on' and 'off' pulse periods. Part of a small but apparent inequality of Q_{on} and Q_{off} of perhaps 20 % can be handled by averaging the two values (Adrian & Almers, 1976*b*). However, when larger conductance changes during the pulse are evident, such averaging will not be an exact measure of the charge moved. In the present study, the equilibrium potential of the delayed rectifier current was likely positive to the holding potential. For pulses showing delayed rectification, this resulted in a large underestimation of Q_{on} ($\sim$ 50 %) and an overestimation of Q_{off} ($\sim$ 100 %), relative to the measurements of Q_{on} performed on the same records corrected for delayed rectification. As pointed out by Adrian & Almers (1976*b*), there is no reason to suppose that these errors will exactly cancel.

Comparison of the kinetics of the outward current and the charge transient

The data correction procedure demonstrates that ΔV_Q and ΔV_K components of ΔV records can be fitted simultaneously if the magnitude of the outward current is small enough not to swamp the charge transient. A comparison of τ_Q and τ_n for fibre F54 is shown in Table 3. In all instances, τ_n (column 4) was greater than τ_Q (column 3). The mean ratio, τ_n/τ_Q was 5·20; this ratio ranged from 2·47 to 8·61 (column 5). The inequality of τ_Q and τ_n demonstrates that the charge transient does not correspond kinetically to dn/dt, under these conditions. This kinetic separation holds equally well for trial fits which assumed that the outward current was proportional to n^2 or n^3; the consistently best fits to ΔV records which showed delayed rectification were obtained using n^4.

Effect of alterations in external Ca^{2+} concentrations on charge movement

Changes in the voltage-dependent properties of muscle charge movement were determined at normal Ca^{2+} concentration, viz. 1·8 mM, and at elevated Ca^{2+} concentrations, viz. 25 mM, 50 mM, or 100 mM. These Ca^{2+} concentrations were chosen as those at which maximal shifts in contraction threshold occurred (*q.v.* Dörrscheidt-

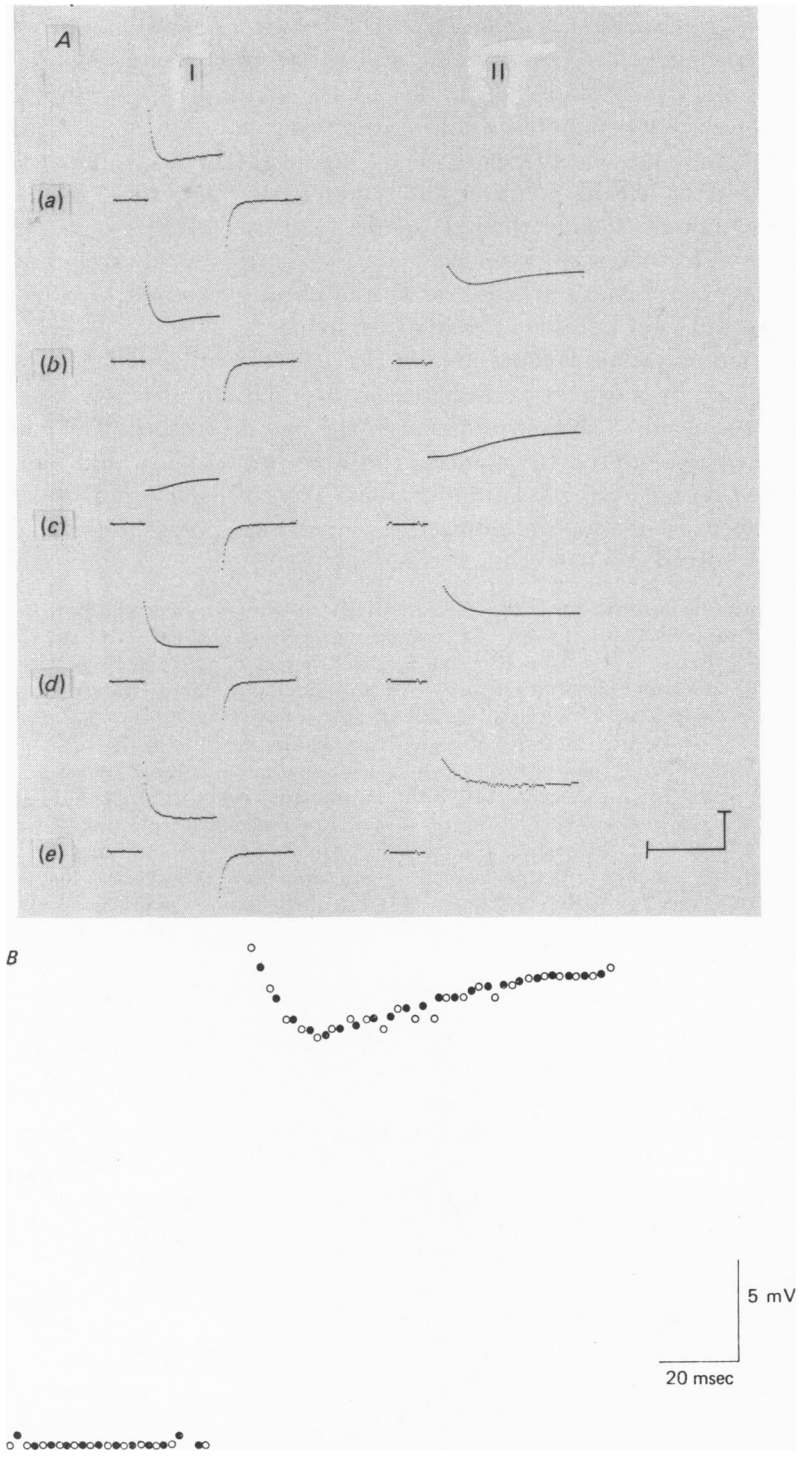

Fig. 6. For legend see facing page.

Käfer, 1976). All calcium experiments were performed in solutions containing either chloride or glucuronate as the major anion (*q.v.*, Table 1, solutions B–I) at pH 7·15.

The preparation was allowed to equilibrate with isosomotic test solution (Table 1, solutions B–E or F–I) for 45 min. The excitability of the preparation was then checked by external stimulation, and the bathing solution was subsequently made three times hypertonic with sucrose and allowed to equilibrate. A total of 1·3–1·7 hr elapsed from the time the preparation was placed into the experimental chamber to the time when the experimental measurements began.

Voltage-clamp experiments designed to examine the effects of alterations in the

TABLE 3. Comparison of time constants of charge and n from fibre F54

1 $[Ca]_o$ (mM)	2 Voltage (mV)	3 τ_Q (msec)	4 τ_n (msec)	5 τ_n/τ_Q	6 Error (mV^2)
50	−3	7·55	65·03	8·61	0·25
50	+15	8·34	20·59	2·47	0·22
100	−2	8·27	59·90	7·25	0·29
100	+8	7·43	63·24	8·51	0·25
100	+17	7·05	42·58	6·04	0·27
100	+27	7·74	20·80	2·69	0·27
100	+30	8·89	28·34	3·19	0·23
100	+50	7·74	21·94	2·83	0·33

Fig. 6. *A*, method of data correction for delayed outward current. All traces were photographed directly from the computer display. Trace *a* represents the raw ΔV record. At this display gain, the first six points of the ΔV record are out of range. Record *a* was fitted in a non-linear least-squares fashion to the general equation: $\Delta V_t = \Delta V_K + \Delta V_Q + W$. For the purpose of illustration, ΔV_Q (trace *d*) and ΔV_K (trace *c*) are displaced along the voltage axis by W, a constant which determined the steady conductance during the voltage pulse. Trace *b* represents the best-fit of the equation for V_t to trace *a* (q.v. Fig. 6*B*). The resultant best-fit parameters were: $\Delta V_Q(\phi) = 23{\cdot}87$ mV; $\tau_Q = 9{\cdot}26$ msec; $\tau_n = 21{\cdot}63$ msec; $\Delta V_K(\infty) = 5{\cdot}85$ mV; and $W = 17{\cdot}61$ mV. The ratio of time constants $\tau_n/\tau_Q = 2{\cdot}34$; the root mean-squared error normalized to the number of points fitted was 0·22. Trace *e* represents the corrected ΔV record. It is formed by point-by-point subtraction of record *c* from record *a*. Records *b*–*e* are shown at higher vertical and horizontal gains in the right column (II).

Fibre reference F56. $(V_2 - V_3)$ was 132·2 mV square pulse; hypertonic solution E; $l = 293{\cdot}7\ \mu$m, $l' = 71{\cdot}2\ \mu$m; 1 mV on ΔV corresponds to 0·035 μA/cm (eqn. (1)). Temperature 4·5 °C.

Calibration bar: Column I, vertical 20 mV, horizontal 100 msec. Column II, vertical 10 mV, horizontal 50 msec.

B, theoretical fit to the raw ΔV record and I_K. Every fifth point of the raw ΔV record (○) shown in *A* is replotted at higher gain. The points during the voltage pulse were fitted to the equation $\Delta V_t = \Delta V_Q + \Delta V_K + W$, where ΔV_Q is the charge movement component, ΔV_K is the outward potassium current component, and W is a constant which determined the steady conductance during the voltage pulse. Every fifth point of the ΔV_t record, the fit (●), is replotted to illustrate the correspondence between the raw ΔV record and its fit. The initial baseline portion of both records have been equated. At this display gain, the first eleven points of the record during the pulse are out of range. ○ Represents the uncorrected ΔV record; ● is the best non-linear least-squares fit to the points during the pulse. Calibration: vertically 5 mV, horizontally 20 msec. See text and *A* for further details.

external Ca^{2+} concentration on membrane charge movement were successfully carried out in more than one test solution on ten fibres from eight muscles. Of these, six fibres from four muscles showed a slow decrease in outward current similar to that previously described. These six fibres, all in solutions with glucuronate as the principle anion, were not analysed.

Effects of increased extracellular Ca^{2+} concentration on charge movement in solutions containing Cl^- as the principle anion

Fig. 7 illustrates the results of the capacitance analysis for each of four runs on fibre F54. The absolute value of the total charge calculated for the pulse 'on' period (open symbols) and the pulse 'off' period (filled symbols), at each voltage,

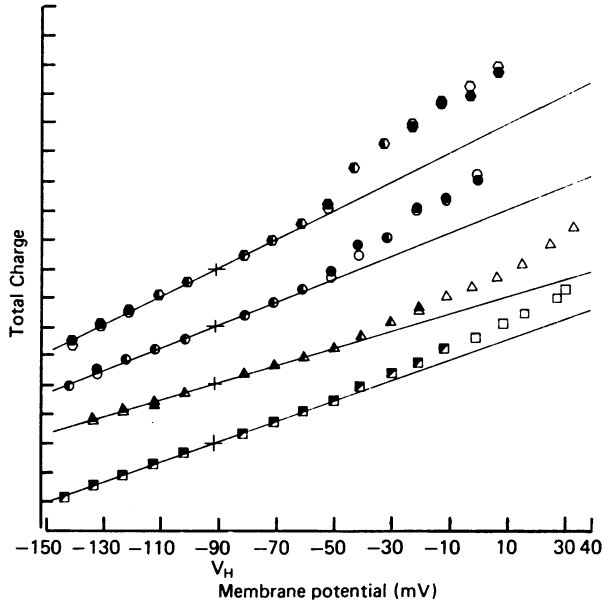

Fig. 7. Relationship between total charge and membrane potential in 1·8 mM, 50 mM, 100 mM, and again in 1·8 mM-$CaCl_2$-containing solutions. The absolute value of the total charge in arbitrary units calculated for the pulse 'on' period, (open symbols) and the pulse 'off' period (filled symbols) is plotted as a function of the steady, calculated V_1 voltage (mV). For corrected ΔV records only the 'on' charge is shown. Each curve is vertically displaced by 100 units for clarity. The continuous lines represent the best linear least-squares fit to the data points negative to the holding potential, V_H, −92 mV. The first measurements were performed in 1·8 mM-Ca^{2+}, solution B (○, ●); the bathing solution was then changed to 50 mM-Ca^{2+}, solution D (△, ▲). Subsequently, the bathing solution was changed to 100 mM-Ca^{2+}, solution E (□, ■) and finally back to 1·8 mM-Ca^{2+}, solution B (○, ●). The electrodes remained within the cell during this sequence and the holding current was low and stable throughout. Solutions B, D and E were made three times hypertonic with sucrose. Fibre F54. The electrodes remained within the cell for these four runs, and the holding current was low and stable throughout.

is plotted as a function of the steady, calculated V_1 voltage. The total charge is expressed in arbitrary units; each run is displaced by 100 units. In this fibre, as in all other fibres, the linear fibre capacitance randomly varied as a function of the Ca^{2+} concentration of the bathing media (*q.v.* Table 4).

A composite graph of the 'extra charge' normalized to the linear fibre capacitance for the four runs on fibre F54 is illustrated in Fig. 8. The continuous curve drawn through each set of data points represents the best non-linear least-squares fit of those data to eqn. (3). Data points derived from the 'on' portion of corrected ΔV records were equally weighted by the curve-fitting procedure with Q_{on} and Q_{off} values derived from uncorrected ΔV records, as previously described.

TABLE 4. Effects of external Ca^{2+} concentration on charge movement. The curve fit parameters, viz. Q_{max} (nC/μF), $\bar{V}$ (mV), k (mV), Error (mV^2), linear fibre capacitance, L.f.c., followed by the cable parameters λ (cm) and r_i (MΩ/cm), head columns IV–X of this Table. The Ca^{2+} concentration and fibre reference are listed in columns I and II. Column III gives the test solution (Table 1) followed by a numeral designating the sequence of the solution change for that fibre. In calculating the grand mean ± S.E. of mean, duplicate runs on the same fibre were averaged so that each fibre was equally weighted as previously described. Fibre F75, run G/2 was done 2·3 hr after run G/1 as a check on the long-term reproducibility

I $[Ca^{2+}]_o$ (mM)	II Fibre	III Solution/ sequence	IV Q_{max} (nC/μF)	V $\bar{V}$ (mV)	VI k (mV)	VII Error (mV^2)	VIII L.f.c.	IX λ (cm)	X r_i (MΩ/cm)
1·8	54	B/1	31·7	−42·5	6·8	0·85	1·98	0·124	11·11
	54	B/4	33·0	−41·4	7·3	1·87	2·46	0·142	15·29
	56	B/1	30·0	−33·5	8·9	1·79	1·93	0·146	19·64
	77	F/3	28·3	−29·2	8·8	1·05	2·18	0·186	9·26
Mean ± S.E. of mean			30·2 ± 1·2	−34·9 ± 3·7	8·3 ± 0·6	—	2·11 ± 0·09	0·155 ± 0·02	14·03 ± 3·02
25	77	G/2	37·2	−5·5	16·8	1·02	2·40	0·244	8·16
	74	G/2	37·3	−23·2	12·4	1·08	2·33	0·159	9·51
	75	G/1	45·8	−11·1	18·5	0·96	2·18	0·173	9·64
	75	G/2	47·2	−14·4	14·7	1·82	2·37	0·113	17·36
Mean ± S.E. of mean			40·3 ± 3·1	−13·8 ± 5·1	15·3 ± 1·4	—	2·34 ± 0·04	0·182 ± 0·03	10·39 ± 1·60
50	54	D/2	34·5	−18·0	14·9	1·48	1·47	0·139	9·98
	56	D/3	34·1	−26·2	17·2	1·46	3·00	0·195	22·33
	74	H/1	38·1	−13·8	11·7	0·95	1·76	0·140	11·19
Mean ± S.E. of mean			35·6 ± 1·3	−19·3 ± 3·6	14·6 ± 1·6	—	2·08 ± 0·47	0·158 ± 0·02	14·5 ± 3·9
100	54	E/3	36·0	+7·4	22·2	1·36	1·75	0·121	12·86
	56	E/2	33·3	−14·5	14·2	1·67	2·42	0·081	21·9
	77	I/1	34·0	+16·9	23·7	1·21	3·18	0·189	8·30
Mean ± S.E. of mean			34·3 ± 0·08	+3·3 ± 9·3	20·0 ± 2·9	—	2·45 ± 0·41	0·130 ± 0·03	14·35 ± 4·0

The curve fit parameters derived for fibre F54 demonstrate a clear shift in the transition voltage, $\bar{V}$, from −42·5 mV in 1·8 mM-Ca^{2+} to −18·0 mV in 50 mM-Ca^{2+} to +7·6 mV in 100 mM-Ca^{2+}. Upon return to 1·8 mM-Ca^{2+}, the $\bar{V}$ parameter returns to its control values, viz. −41·4 mV. There is a slight increase in the apparent Q_{max} from 31·7 nC/μF in 1·8 mM-Ca^{2+} to 34·5 nC/μF in 50 mM-Ca^{2+} and 36·0 nC/μF in 100 mM-Ca^{2+}; this is probably not significant.

The derived k parameter increases with increasing extracellular Ca^{2+} concentration from 6·8 mV in 1·8 mM-Ca^{2+} to 14·9 mV in 50 mM-Ca^{2+}, and 22·2 mV in

100 mM-Ca^{2+}. Upon return to 1·8 mM-Ca^{2+}, the k parameter returns to approximately its control value, viz. 7·3 mV.

The charge movement parameters for other fibres are tabulated in Table 4.

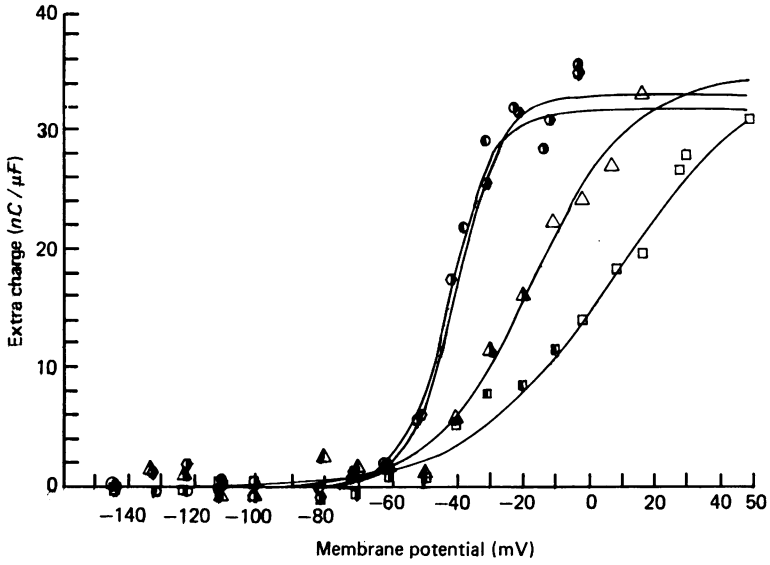

Fig. 8. Steady-state charge normalized to fibre capacitance in 1·8 mM, 50 mM, 100 mM, and again in 1·8 mM-$CaCl_2$-containing solutions. Charge displacements were obtained by averaging, except for corrected records, the 'extra charge' determined for the pulse 'on' and pulse 'off' periods for each of the four runs on fibre F54. In this as in all subsequent composite Q–V curves, the average value of the 'extra charge' measured for the pulse 'on' and pulse 'off' periods is denoted by half-filled symbols. Values for Q_{on} determined on ΔV records corrected for delayed rectification are denoted by open symbols. The curves were drawn according to eqn. (3) which was fitted to the averaged data points for uncorrected records and to the 'on' data points for corrected records at voltages more positive than the holding potential, −92 mV. The best fit parameters are shown below.

Best-fit parameters for fibre F54

Run	$[Ca]_o$ (mM)	Q_{max} (nC/μF)	$\bar{V}$ (mV)	k (mV)	Error (mV^2)
1 (○)	1·8	31·7	−42·5	6·8	0·85
2 (△)	50·0	34·5	−18·0	14·9	1·48
3 (□)	100·0	36·0	+7·6	22·2	1·36
4 (○)	1·8	33·0	−41·4	7·3	1·87

Effects of increased extracellular Ca^{2+} concentration on charge movement in solutions containing glucuronate as the principle anion

To eliminate the possibility that voltage- and time-dependent changes in chloride conductance at neutral pH (Hutter & Warner, 1972; Warner, 1972) contributed to the observed shifts in the Q–V curve as the external Ca^{2+} concentration of the bathing medium was raised, a series of experiments were performed in solutions containing glucuronate as the principle anion. In contrast to chloride, which contributes approximately 66% of the resting fibre conductance (Adrian & Freygang,

1962), glucuronate is relatively impermeable. Before the experimental measurements were begun, the fibres were equilibrated for 1 hr with isosmotic solution F (*q.v.* Table 1), in order to allow the internal Cl^- to wash out.

The charge movement parameters for fibre F77 are in Table 4. Following an initial run in 100 mM-Ca^{2+} (solution I), the charge movement properties of this fibre were measured in 25 mM-Ca^{2+} (solution G), and finally in 1·8 mM-Ca^{2+} (solution F). Solutions I, G, and F were made three times hypertonic with sucrose. The $\bar{V}$ parameter shifted from +16·9 mV in 100 mM-Ca^{2+} to −5·5 mV in 25 mM-Ca^{2+} and −29·2 mV in 1·8 mM-Ca^{2+}. This result is in qualitative agreement with results reported earlier (for fibre F54 (Fig. 8)), for changing external Ca^{2+} concentration when Cl^- was the principle solution anion. The k parameter, which fell as the Ca^{2+} concentration was lowered, ranged from 23·7 mV in 100 mM-Ca^{2+} to 16·8 mV in 25 mM-Ca^{2+} and 8·8 mV in 1·8 mM-Ca^{2+}. The maximum amount of charge, Q_{max}, rose slightly from 34·0 nC/μF in 100 mM-Ca^{2+} to 37·2 nC/μF in 25 mM-Ca^{2+}. It then decreased to 28·3 nC/μF in 1·8 mM-Ca^{2+}. Q_{max} always was at least as great as that measured in 1·8 mM-Ca^{2+}. No significant change in the linear fibre capacitance was observed over the range of 1·8–100 mM-Ca^{2+} solution where glucuronate was the principle anion.

Summary of calcium effects

The results of the calcium experiments demonstrate a shift in the transition potential, $\bar{V}$, along the voltage axis in the depolarizing direction. The 21·1 mV shift in $\bar{V}$ from means of −34·9 mV in 1·8 mM-Ca^{2+} to −13·8 mV in 25 mM-Ca^{2+} is statistically significant ($0{\cdot}02 < \alpha < 0{\cdot}05$). The mean 15·6 mV shift in $\bar{V}$ parameter between −34·9 mV in 1·8 mM-Ca^{2+} and −19·3 mV in 50 mM-Ca^{2+} is significant ($0{\cdot}02 < \alpha < 0{\cdot}05$), as is the mean 38·2 mV shift in $\bar{V}$ measured between 1·8 and 100 mM-Ca^{2+} ($0{\cdot}01 < \alpha < 0{\cdot}02$).

The shift in the parameter k from a mean of 8·3 mV in 1·8 mM-Ca^{2+} relative to means of 15·3 mV ($0{\cdot}01 < \alpha < 0{\cdot}02$) in 25 mM-$Ca^{2+}$, 14·6 mV ($0{\cdot}02 < \alpha < 0{\cdot}05$) in 50 mM-$Ca^{2+}$, and 20·0 mV ($0{\cdot}02 < \alpha < 0{\cdot}05$) in 100 mM-$Ca^{2+}$, are each statistically significant at the indicated levels. Essentially the same k value was obtained from semi-log plots using data obtained from the foot of the 'extra-charge' *vs.* voltage curves.

On the other hand, changes in the linear fibre capacitance in 1·8 mM-Ca^{2+} relative to 25, 50 and 100 mM-Ca^{2+} are not significantly different.

Effects of 4-aminopyridine on the contraction threshold

The just-detectable contraction threshold was measured in ten fibres from a semitendinosus muscle to determine the effect of 4-aminopyridine on the contraction threshold. The measurements were performed using a two micro-electrode voltage-clamp technique (Costantin, 1968). The just-detectable contraction threshold was determined visually through the dissecting microscope. At a fixed 95 msec pulse duration, the pulse amplitude was increased in 5 mV steps from the holding potential, −90 mV, until contraction was noticed. The amplitude was decreased by 10 mV, and increased in 1 mV steps until contraction was again just detected. The interval between pulses was about 20 sec. The sequence was repeated four times;

the average potential was taken as the just-detectable contraction threshold. After an initial series of measurements in isotonic solution A and 10^{-6} g TTX/ml. (Table 1), the bathing solution was changed to a similar solution plus 1 mM-4-aminopyridine. After 1 hr equilibration, the measurements were repeated. The bathing solution was changed back to solution A plus 10^{-6} g TTX/ml. without 4-aminopyridine, allowed to equilibrate for 1 hr, and a third set of measurements were performed. The resultant contraction thresholds were: $-39{\cdot}7 \pm 1{\cdot}6$ mV in the absence of 4-aminopyridine; $-39{\cdot}1 \pm 2{\cdot}6$ mV in the presence of 1 mM-4-aminopyridine; and $-36{\cdot}0 \pm 2{\cdot}9$ mV after 1 hr re-equilibration in 4-aminopyridine-free solution. During the last run, a fibre, included in the mean, showed a shift in its contraction threshold to -15 mV. Discounting this fibre, the mean result for the third run is $-38{\cdot}3 \pm 1{\cdot}9$ mV. None of these changes in the contraction threshold are significantly different ($\alpha > 0{\cdot}5$).

DISCUSSION

A comparison of the present results with previous results

Charge movement parameters at pH 7·15 in 1·8 mM-Ca^{2+} from the present study are compared with published results in Table 5.

In the present study, there is no statistically significant difference between $\bar{V}$ parameters determined at pH 7·15, 1·8 mM-Ca^{2+} in solutions containing glucuronate, Cl^-, or SO_4^{2-} as the principle anionic constituent ($\alpha > 0{\cdot}5$). Variations in Q_{max} and the small changes in the parameter k, measured in solutions containing glucuronate or SO_4^{2-}, are not significant ($0{\cdot}5 < \alpha < 0{\cdot}1$). In all other comparisons, no significant differences were detected ($\alpha > 0{\cdot}3$).

The results from all experiments at pH 7·15 in 1·8 mM-Ca^{2+} are shown in column 9 of Table 5. In comparing all results (column 9) with published data, the Q_{max} parameter is clearly more consistent with the results obtained by Adrian & Almers (1976*b*). The mean k parameter is approximately midway between the results of Chandler *et al.* (1976*a*) and those of Adrian & Almers (1976*b*). From the mean k, an apparent valence for the particle is calculated as $\approx 2{\cdot}7 \pm 0{\cdot}02$ (*q.v.* Methods: calculation of extra charge).

However, in the present study, the mean transition voltage, $\bar{V}$, viz. $-35{\cdot}8 \pm 1{\cdot}5$ mV, was found to be approximately 10 mV more depolarized than in the previous studies. The only exception is fibre F54 (*q.v.* Table 4) where the difference in $\bar{V}$ was somewhat less, approximately 6 mV. The reason for this discrepancy is not immediately clear. The only major difference in conditions in the present study was the addition of 1 mM-4-aminopyridine to further reduce delayed rectification. However, the contraction threshold, $-39{\cdot}1 \pm 2{\cdot}6$ mV, measured in the presence of 4-aminopyridine, was not significantly different from that measured, viz. $-39{\cdot}7 \pm 1{\cdot}6$ mV and $-36{\cdot}0 \pm 2{\cdot}9$ mV, in the absence of 4-aminopyridine. The contraction threshold for 95 msec pulses reported in the present study was also found to be approximately 9 to 10 mV more depolarized, in comparison with values reported by others. Chandler *et al.* (1976*b*) reported a contraction threshold of $-48{\cdot}3 \pm 1{\cdot}7$ mV in similar chloride-containing solution without 4-aminopyridine. This latter result is also consistent with the $-48{\cdot}5$ mV threshold observed by Costantin (1968). A difference in the temperature or another physiological state of the frogs may account for part of this

TABLE 5. In *A*, column 1 gives the curve fit and cable parameters, columns 2 and 3 give the mean results obtained in the series of pH experiments, and columns 4 and 5 give the mean results obtained in the series of calcium experiments. The pH experiments were performed on fibres from room-temperature adapted, fed frogs using solutions containing either glucuronate or sulphate as the principle anion. The calcium experiments were performed on fibres from cold-adapted, unfed frogs using solutions containing either glucuronate or chloride as the principle anion. Columns 6–9 summarize all results obtained at pH 7·15 in 1·8 mM-Ca^{2+} solutions containing glucuronate, chloride, sulphate, or combinations, as the principle anion, respectively. Column 10 summarizes experiments using room-temperature adapted frog fibres while column 11 summarizes experiments performed on cold-adapted frog fibres.

In *B* are summarized published data in similar solutions containing either chloride or sulphate as the principle anion. The charge movement properties of muscle cells have not previously been measured in solutions containing glucuronate as the principle anionic constituent.

A. Charge movement parameters at pH 7·15 in 1·8 mM-Ca^{2+}

1	2	3	4	5	6	7	8	9	10	11
Condition	pH experiments		Ca^{2+} experiments		All results				All pH experiments	All Ca^{2+} experiments
Anion	Glucuronate	Sulphate	Glucuronate	Chloride	Glucuronate	Chloride	Sulphate	All	All	All
Parameters										
Q_{max} (nC/μF)	34·3 ± 1·2	21·6	28·3	31·6 ± 0·7	32·8 ± 1·7	31·6 ± 0·8	21·6	30·9 ± 1·8	31·1 ± 3·3	30·2 ± 1·2
$\bar{V}$ (mV)	−35·9 ± 0·9	−38·2	−29·2	−37·8 ± 4·2	−34·4 ± 1·8	−37·8 ± 4·3	−38·2	−35·8 ± 1·5	−36·5 ± 0·9	−34·9 ± 3·7
k (mV)	10·1 ± 0·8	8·6	8·8	8·0 ± 0·9	10·2 ± 0·7	8·0 ± 0·9	8·6	9·3 ± 0·6	10·2 ± 0·8	8·3 ± 0·6
λ (cm)	0·102 ± 0·02	0·224	0·126	0·140 ± 0·01	0·083 ± 0·02	0·040 ± 0·01	0·224	0·134 ± 0·02	0·133 ± 0·03	0·155 ± 0·01
r_i (MΩ/cm)	11·63 ± 0·42	8·30	9·26	16·42 ± 3·2	11·04 ± 0·66	16·42 ± 3·2	8·3	12·18 ± 1·39	11·91 ± 1·4	14·03 ± 3·02
N	3	1	1	2	4	2	1	7	4	3

B. Published charge movement parameters in 1·8 mM-Ca^{2+}

Condition	Q_{max} (nC/μF)	$\bar{V}$ (mV)	k (mV)	Reference
Chloride	24·5 ± 1·7	−44·1 ± 3·4	7·8 ± 0·7	Chandler *et al.* 1976*a*
Sulphate	32·0 ± 3·0	−48·6 ± 2·6	12·6 ± 1·5	Adrian & Almers, 1976*b*

discrepancy. The difference in $\bar{V}$ which was seen in 1·8 mV-Ca^{2+} solutions with Cl^-, glucuronate, or SO_4^{2-} as the major anion is clearly not an anion effect.

Since seasonal variations in passive electrical properties of toad muscle fibres (Dulhunty & Gage, 1973) and in the contractile behaviour of frog fibres (Kovács & Schneider, 1977) have been reported, it was of interest to see if there was a corresponding effect on charge movement. To investigate this variation, the charge movement properties of muscle fibres from room-temperature adapted and cold-adapted frogs were compared. This was done by comparing the mean curve fit parameters obtained in the pH series of experiments in 1·8 mM-Ca^{2+} at pH 7·15 (Table 5, column 10) with the mean results from the calcium experiments (column 11) which were performed under similar experimental conditions. Changes in the derived k ($0{\cdot}1 < \alpha < 0{\cdot}2$), Q_{max} ($\alpha > 0{\cdot}5$) and $\bar{V}$ ($\alpha > 0{\cdot}5$) parameters are not significantly different from different populations of frogs adapted to a room-temperature or cold environment. Dulhunty & Gage (1973) reported a 70 % increase in the space constant of single fibres from summer toads compared to winter toads. However, in the present study, no significant difference in either λ ($\alpha > 0{\cdot}5$) or r_i ($0{\cdot}2 < \alpha < 0{\cdot}3$) was observed from fibres of room-temperature or cold-adapted frogs. The discrepancy may in part be explained by assuming that the winter toads used by Dulhunty & Gage (1973) were in a different physiological state than the cold-adapted frogs used in this study.

Adrian & Almers (1976*b*), who examined the effects of reduced Ca^{2+} concentration (2 mM-$CaSO_4$) on charge movement parameters in different fibres, observed no significant differences relative to control measurements (8 mM-$CaSO_4$). The results reported in this study were generally performed on the same fibre for both test and control measurements, to reduce fibre to fibre variability, and demonstrate significant changes in both $\bar{V}$ and k as a function of external calcium concentration. Experiments designed to investigate the effects of elevated external Ca^{2+} concentration and the effects of changes in external pH have not previously been reported.

Effects of pH on charge movement

The observed $\sim$ 16 mV shift (*q.v.* Table 2) in the mean transition voltage, $\bar{V}$, from $-42{\cdot}5 \pm 1{\cdot}8$ mV at pH 9 to $-25{\cdot}8 \pm 1{\cdot}3$ mV at pH 5·5 is generally consistent in direction, but not in magnitude, with shifts in the contraction threshold with changing pH (Dörrscheidt-Käfer, 1976). Dörrscheidt-Käfer did not measure the effect of pH on contraction threshold at 1·8 mM-Ca^{2+}; she used either reduced (0·5 mM) or elevated (5 or 50 mM) Ca^{2+} concentrations. In 0·5 mM-Ca^{2+}, she observed a threshold shift of approximately 24·1 mV in a depolarizing direction upon changing from pH 10·3 to 4·65. In 5 mM-Ca^{2+}, only a 12 mV shift of the contraction threshold was observed for a similar change in pH.

The results reported in this study for changes in external pH from 9 to 5·5 are approximately midway within the range of Dörrschedit-Käfer's (1976) observations. Consistent with simple surface charge theory, no significant changes in the k or Q_{max} parameters were observed over the range pH 5·5–9·0. The mean k values of $10{\cdot}2 \pm 0{\cdot}8$ mV at pH 7·15 gives rise to an average effective particle valence of $\approx 2{\cdot}5 \pm 0{\cdot}2$. The effect of pH on the charge movement parameter, $\bar{V}$, observed in these experiments and the changes in contraction threshold reported by Dörrscheidt-

Käfer (1976) are clearly qualitatively consistent. This observation coupled with clear kinetic separations of τ_Q and τ_n (Table 3) adds further support to the hypothesis that the charge movement is involved in gating muscle contraction and that the charged particles respond to changes in the electric field across the membrane.

Effects of calcium on charge movement

In the present study, the mean transition potential, $\bar{V}$, shifted approximately 16 mV in a depolarizing direction when the external Ca^{2+} concentration was raised from 1·8 to 50 mM (Table 4). This result is in agreement in both direction and magnitude with reported shifts in the contraction threshold of 19 mV at pH 7·2 (Costantin, 1968, Fig. 2), and approximately 22 mV at pH 6·5 (Dörrscheidt-Käfer & Lüttgau, 1974) for the same change in Ca^{2+} concentration. At pH 7·15, Dörrscheidt-Käfer (1976, Fig. 1) showed an approximately 36 mV shift in the contraction threshold for the 100-fold increase from 0·5 mM to 50 mM in calcium concentration. However, in the present study, only a fifty-six-fold increase from 1·8 mM- to 100 mM-Ca^{2+}, produced a 38 mV shift. The variance of the findings from the results reported in this study is likely to be due to the different experimental conditions required to measure charge movement: Dörrscheidt-Käfer (1976) used TTX, and the present study was conducted in the presence of TTX, TEA, rubidium, and 4-aminopyridine, and in solutions made three times hypertonic with sucrose.

In contrast to the pH experiments, in the calcium experiments the parameter k progressively increased as the Ca^{2+} concentration was raised. The increase in k reflects a decrease in the effective particle valence from $\approx 3{\cdot}0 \pm 0{\cdot}2$ in 1·8 mM-Ca^{2+} to $\approx 1{\cdot}6 \pm 0{\cdot}2$, $\approx 1{\cdot}7 \pm 0{\cdot}2$ and $\approx 1{\cdot}2 \pm 0{\cdot}2$ in 25, 50 and 100 mM-Ca^{2+} respectively. The 43 % decrease in the apparent valence suggests a specific interaction between external Ca^{2+} ions and the charge movement. This interaction may be separate and distinct from the shifts in the parameter $\bar{V}$ which were observed as pH was decreased or as the Ca^{2+} concentration was increased. These changes in $\bar{V}$, consistent with surface charge theory, are due to increases in the membrane electric field.

The shifts in $\bar{V}$ obtained in the series of calcium experiments seemed consistent with a fixed charge of one negative electronic charge, e, per 140–200 Å^2 and no calcium binding. The shifts in $\bar{V}$ data in 25 and 50 mM-Ca^{2+} solutions, possibly due to a glucuronate effect, are such that only an approximate value for surface charge can be found. The range of values for fixed charge is in the range of the effective surface charge density, viz. $-1e/120$ Å^2 calculated from Dörrscheidt-Käfer (1976) results. Although the effects of k *vs.* external Ca^{2+} concentration can be explained by a simple binding scheme where one divalent cation binds to a triple negatively charged group with an association constant of 50 mM, the relative constancy of Q_{max} is not explained. Although there is no apparent explanation, the results tend to rule out the idea that the effects of divalent ions on gating particles can be explained by a simple shift in potential alone (Rojas & Keynes, 1975).

The shifts in $\bar{V}$ parameter observed in the pH experiments were examined using surface charge theory (Begenisich, 1974). A fairly resaonable fit to the data over the range of pH 5·5–9 could be obtained with two pK values: $\sigma_1 = -1e/165$ Å^2, $pK_1 = 3{\cdot}9$ and $\sigma_2 = -1e/400$ Å^2, $pK_2 = 8$ (Fig. 9). A basic pK of $\sim 8{\cdot}5$ was found necessary by Dörrscheidt-Käfer (1976). Similarly basic pK values were

necessary to explain surface charge effects in nerve (Hille, 1968; Mozhayeva & Naumov, 1972; Hille, Woodhull & Shapiro, 1975).

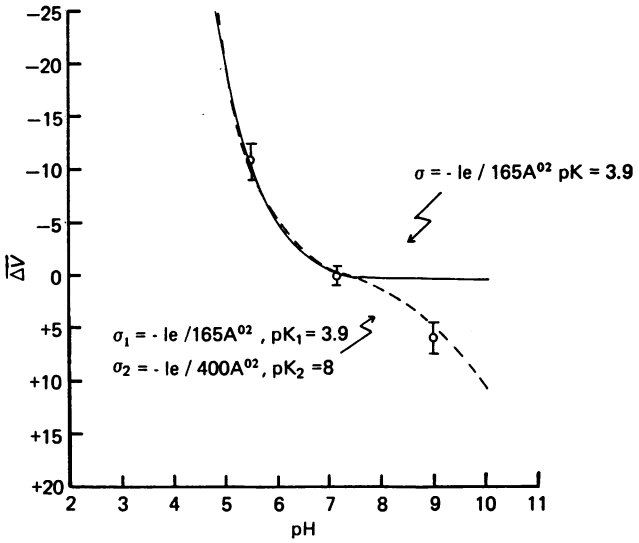

Fig. 9. Shifts in the charge movement parameter $\bar{V}$ and pH. The average value of the shifts in $\bar{V}$ from the pH experiment is plotted against the external pH. The values have been referenced to the mean $\bar{V}$ obtained at pH 7·15.

The continuous line represents the best-fit of the Grahame equation to the experimental data obtained using a single acidic pK of 3·9 and surface charge density of $-1e/165$ Å^2. A clearly better fit over the range pH 5·5 to pH 9 is shown by the dashed line using two pK values: $\sigma_1 = -1e/165$ Å^2, $pK_1 = 3{\cdot}9$, and $\sigma_2 = -1e/400$ Å^2, $pK_2 = 8$.

Open circles are averages (±S.E. of mean) of the experimental data.

Importance of the correction procedure

The correction procedure is important because it removes an ionic current during the voltage pulse. Therefore, the 'on' area measured on corrected ΔV records was uncomplicated by a significant ionic current, and is valid. As discussed earlier, no correction to the 'off' portion of the ΔV records could be performed, and therefore no internal check of Q_{on} and Q_{off} was possible. In one fibre, F56, small outward currents on ΔV records were evident at -10 and 0 mV in 1·8 mM-Ca^{2+}. The analysis of these records after correction resulted in values for Q_{on} consistent with the individual Q_{on} and Q_{off} values or their averages at more negative potentials using uncorrected data on this same fibre. It is important to note that the potential range over which the correction was necessary was usually beyond the transition potential of the Q–V curve. Since eqn. (3) used to fit the Q–V curves is symmetric about $\bar{V}$, only knowledge of data just beyond the mid-point is necessary to define the relationship unambiguously.

The changes in membrane conductance which were observed in the test solutions are not entirely unexpected. A number of factors which contributed to the observed outward current, and therefore, need to be considered are as follows. (1) In solutions containing a normal Ca^{2+} concentration, i.e. 1·8 mM (solutions B, F, and J, Table 1) the increase in ionic current during

a large depolarizing test pulse might be due to the slow K conductance change described by Adrian *et al.* (1970*b*), which is relatively ressitant to blockage by TEA ions (Kao & Stanfield, 1970; Stanfield, 1970*a*, *b*). (2) TEA ions at a concentration of 58 mM shift the threshold for the onset of delayed rectification to more negative membrane potentials (Costantin, 1968; Stanfield, 1970*a*) and increase its apparent time constant (Stanfield, 1970*a*). In the presence of the twofold higher concentration of TEA used in these experiments, i.e. 117·5 mM, the threshold for the onset of delayed rectification would be expected to shift still further in the hyperpolarizing direction, and therefore might further compound the ineffectiveness of the TEA block of outward potassium current. (3) In experimental solutions with elevated external free Ca^{2+} concentrations, viz. 25, 50, or 100 mM, the membrane conductance increase during the test pulse was larger in magnitude than the much smaller increase in conductance that was seen at the end of an equivalent voltage pulse in 1·8 mM-Ca^{2+}. On increasing the external Ca^{2+} concentration, a similar reduction in the effectiveness of TEA ion blockage of outward potassium currents was observed in the membrane of the node of Ranvier of the frog by Mozhayeva & Naumov (1972) who explained their results by assuming that the increased extracellular calcium reduced the negative surface potential and thereby reduced the concentration of TEA ions at the membrane surface by a factor of 1·61 for a tenfold change in Ca^{2+} concentration. Other independent factors known to influence surface charge (Chandler, Hodgkin & Meves, 1965; Hille, 1968) gave similar results which were also consistent with surface charge theory (Mozhayeva & Naumov, 1972). (4) The use of 1 mM-4-aminopyridine, which is believed to act from the interior of the fibre, to further block delayed potassium currents (Gillespie & Hutter, 1975; Meves & Pichon, 1975; Ulbricht & Wagner, 1975; Yeh, Oxford, Wu & Harahashi, 1976) was not totally satisfactory.

The author is especially grateful to Dr Martin F. Schneider for his invaluable advice and helpful discussion throughout the course of this work. In addition, the author wishes to thank Drs R. H. Adrian, T. B. Begenisich, P. Horowicz, P. G. Shrager and R. Kilpper for much helpful discussion. Dr R. F. Rakowski very kindly provided the curve-fitting programmes for potassium currents; and Dr S. Baylor provided a data acquisition routine. The author is particularly grateful to his wife who helped prepare the illustrations and to Mrs Luanne Wussow for typing the manuscript. This has been work submitted to and accepted by the Faculty of the University of Rochester in partial fulfilment of the requirements for the Ph.D. degree in Physiology. The author was supported by the NIH-USPHS (GM 00394) and by the University of Rochester. The author thanks Drs M. F. Schneider, R. F. Rakowski and S. R. Taylor for criticisms of this manuscript.

REFERENCES

ADRIAN, R. H. & ALMERS, W. (1976*a*). The voltage dependence of membrane capacity. *J. Physiol.* **254**, 317–605.

ADRIAN, R. H. & ALMERS, W. (1976*b*). Charge movement in the membrane of striated muscle. *J. Physiol.* **254**, 339–360.

ADRIAN, R. H., CHANDLER, W. K. & HODGKIN, A. L. (1966). Voltage clamp experiments in skeletal muscle fibres. *J. Physiol.* **186**, 51–52*P*.

ADRIAN, R. H., CHANDLER, W. K. & HODGKIN, A. L. (1969). The kinetics of mechanical activation in frog muscle. *J. Physiol.* **204**, 207–230.

ADRIAN, R. H., CHANDLER, W. K. & HODGKIN, A. L. (1970*a*). Voltage clamp experiments in striated muscle fibres. *J. Physiol.* **208**, 607–644.

ADRIAN, R. H., CHANDLER, W. K. & HODGKIN, A. L. (1970*b*). Slow changes in potassium permeability in skeletal muscle. *J. Physiol.* **208**, 645–668.

ADRIAN, R. H., COSTANTIN, L. L. & PEACHEY, L. D. (1969). Radial spread of contraction in frog muscle fibres. *J. Physiol.* **204**, 231–257.

ADRIAN, R. H. & FREYGANG, W. H. (1962). The potassium and chloride conductance of frog muscle membrane. *J. Pyhsiol.* **163**, 61–103.

ARMSTRONG, C. M. & BEZANILLA, F. (1973*a*). Currents related to movement of the gating particles of sodium channels. *Nature, Lond.* **242**, 459–461.

ARMSTRONG, C. M. & BEZANILLA, F. (1973*b*). Properties of gating currents of sodium channels. *Biol. Bull. mar. biol. Lab., Woods Hole* **143**, 423.

ARMSTRONG, C. M. & BEZANILLA, F. (1974). Charge movement associated with the opening and closing of the activation gates of Na channels. *J. gen. Physiol.* **63**, 533–542.

BAYLOR, S. M. & OETLIKER, H. (1977*a*). A large birefringence signal preceding contraction in single twitch fibres of the frog. *J. Physiol.* **264**, 141–162.

BAYLOR, S. M. & OETLIKER, H. (1977*b*). The optical properties of birefringence signals from single muscle fibres. *J. Physiol.* **264**, 163–198.

BAYLOR, S. M. & OETLIKER, H. (1977*c*). Birefringence signals from the surface and T-system membranes of frog single muscle fibres. *J. Physiol.* **264**, 199–213.

BEGENISICH, T. B. (1974). The magnitude and location of fixed charges in *Myxicola* giant axons. Doctoral Dissertation, University of Maryland.

BEZANILLA, F. & ARMSTRONG, C. M. (1975). Kinetic properties and inactivation of the gating currents of sodium channels in squid axon. *Phil Trans. R. Soc. B.* **270**, 449–458.

BEZANILLA, F., CAPUTO, C. & HOROWICZ, P. (1972). Voltage activation of contraction in single fibers of frog striated muscle. *J. physiol. Soc. Japan.* **34**, 1.

BEZANILLA, F. & HOROWICZ, P. (1975). Fluorescence intensity changes associated with contractile activation in frog muscle stained with Nile Blue A. *J. Physiol.* **246**, 709–735.

CHANDLER, W. K., HODGKIN, A. L. & MEVES, H. (1965). The effect of changing the internal solution on sodium inactivation and related phenomena in giant axons. *J. Physiol.* **180**, 821–836.

CHANDLER, W. K., RAKOWSKI, R. F. & SCHNEIDER, M. F. (1976*a*). A non-linear voltage dependent charge movement in frog skeletal muscle. *J. Physiol.* **254**, 245–283.

CHANDLER, W. K., RAKOWSKI, R. F. & SCHNEIDER, M. F. (1976*b*). Effects of glycerol treatment and maintained depolarization on charge movement in skeletal muscle. *J. Physiol.* **254**, 285–316.

COSTANTIN, L. L. (1968). The effect of calcium on contraction and conductance thresholds in frog skeletal muscle. *J. Physiol.* **195**, 119–132.

COSTANTIN, L. L. (1970). The role of sodium current in the radial spread of contraction in frog muscle fibers. *J. gen. Physiol.* **55**, 703–715.

DÖRRSCHEIDT-KÄFER, M. (1976). The action of Ca^{2+}, Mg^{2+}, and H^+ on the contraction threshold of frog skeletal muscle: evidence for surface charges controlling electromechanical coupling. *Pflügers Arch.* **362**, 33–41.

DÖRRSCHEIDT-KÄFER, M. & LÜTTGAU, H. C. (1974). The effect of lanthanum ions on mechanical threshold and potassium contractures in frog skeletal muscle fibres. *J. Physiol.* **242**, 101–102*P*.

DULHUNTY, A. F. & GAGE, P. W. (1973). Electrical properties of toad sartorius muscle fibres in summer and winter. *J. Physiol.* **230**, 619–641.

DYDYŃSKA, M. & WILKIE, D. R. (1963). The osmotic properties of striated muscle fibres in hypertonic solutions. *J. Physiol.* **169**, 312–329.

EBASHI, S., ENDO, M. & OHTSUKI, I. (1969). Control of muscle contraction. *Q. Rev. Biophys.* **2**, 351–384.

FALK, G. (1968). Predicted delays in the activation of the contractile system. *Biophys. J.* **8**, 608–625.

FRANZINI-ARMSTRONG, C. (1970). Studies of the triad. I. Structure of the junction in frog twitch fibers. *J. Cell Biol.* **47**, 488–499.

FRANZINI-ARMSTRONG, C. (1971). Studies of the triad. II. Penetration of tracers into the junctional gap. *J. Cell Biol.* **49**, 196–203.

FRANZINI-ARMSTRONG, C. (1975). Membrane properties and transmission at the triad. *Fedn. Proc.* **34**, 1382–1389.

GILLESPIE, J. I. & HUTTER, O. F. (1975). The actions of 4-aminopyridine on the delayed potassium current in skeletal muscle fibers. *J. Physiol.* **252**, 70–71*P*.

HILLE, B. (1968). Charges and potentials at the nerve surface: divalent ions and pH. *J. gen. Physiol.* **51**, 199–219.

HILLE, B., WOODHULL, A. M. & SHAPIRO, B. I. (1975). Negative surface charge near sodium channels of nerve: divalent ions, monovalent ions and pH. *Phil. Trans. R. Soc. B.* **270**, 301–318.

HODGKIN, A. L. & HOROWICZ, P. (1957). The differential action of hypertonic solutions on the twitch and action potential of a muscle fibre. *J. Physiol.* **136**, 17*P*.

HODGKIN, A. L. & HOROWICZ, P. (1959). The influence of potassium and chloride ions on the membrane potential of single muscle fibres. *J. Physiol.* **148**, 127–160.

HUTTER, O. F. & WARNER, A. E. (1967). The pH sensitivity of the chloride conductance of frog skeletal muscle. *J. Physiol.* **189**, 403–425.

HUTTER, O. F. & WARNER, A. E. (1972). The voltage dependence of the chloride conductance of frog muscle. *J. Physiol.* **227**, 275–290.

HUXLEY, A. F. & STRAUB, R. W. (1958). Local activation and interfibrillar structures in striated muscle. *J. Physiol.* **143**, 40*P*.

HUXLEY, A. F. & TAYLOR, R. E. (1958). Local activation of striated muscle fibres. *J. Physiol.* **144**, 426–441.

KAO, C. Y. & STANFIELD, P. R. (1970). Actions of some cations on the electrical properties and mechanical threshold of frog sartorius muscle fibers. *J. gen. Physiol.* **55**, 620–639.

KOVÁCS, L. & SCHNEIDER, M. F. (1977). Increased optical transparency associated with excitation-contraction coupling in voltage-clamped cut skeletal muscle fibres. *Nature, Lond.* **265**, 556–560.

LÜTTGAU, H. C. (1963). The action of calcium ions on potassium contractures of single muscle fibres. *J. Physiol.* **168**, 679–697.

MEVES, H. & PICHON, Y. (1975). Effects of 4-aminopyridine on the potassium current in internally perfused giant axons of the squid. *J. Physiol.* **251**, 60–62*P*.

MOZHAYEVA, G. N. & NAUMOV, A. P. (1972). Tetraethylammonium ion inhibition of potassium conductance of the nodal membrane. *Biochim. biophys. Acta.* **290**, 248–255.

ROBINSON, R. A. & STOKES, R. H. (1970). *Electrolyte Solutions. The Measurement and Interpretation of Conductance, Chemical Potential and Diffusion in Solutions of Simple Electrolytes.* London: Butterworth & Co.

ROJAS, E. & KEYNES, R. D. (1975). On the relation between displacement currents and activation of the sodium conductance in the squid axon. *Phil. Trans. R. Soc. B.* **270**, 459–482.

SANDOW, A. (1965). Excitation-contraction coupling in skeletal muscle. *Pharmac. Rev.* **17**, 265–320.

SCHNEIDER, M. F. & CHANDLER, W. K. (1973). Voltage dependent charge movement in skeletal muscle: a possible step in excitation-contraction coupling. *Nature, Lond.* **242**, 244–246.

SCHNEIDER, M. F. & CHANDLER, W. K. (1976). Effects of membrane potential on the capacitance of skeletal muscle fibers. *J. gen. Physiol.* **67**, 125–163.

SHLEVIN, H. (1976). An adaptable modular data collection system suitable for scientific experimentation: analog to digital transformation, short term digital storage, formatted digital tape recording, and computer entry of experimental data. *Proc. Am. Fedn Inf. Proc. Soc.* **45**, 295–300.

SHLEVIN, H. H. (1977). Effects of external calcium concentration and pH on intramembrane charge movement in the semitendinosus muscle of the frog, *Rana pipiens*. Doctoral Dissertation. University of Rochester, Rochester, New York.

SHLEVIN, H. H. (1978). Effects of external Ca^{2+} and pH on muscle charge movement. *Biophys. J.*, **21**, 168 *a*.

SIGMA CHEMICAL CO. (1972). *Trizma. Technical Bulletin No.* 106 *B*. St. Louis, Missouri:

STANFIELD, P. R. (1970*a*). The effect of the tetraethylammonium ion in the delayed currents of frog skeletal muscle. *J. Physiol.* **209**, 209–229.

STANFIELD, P. R. (1970*b*). The differential effects of tetraethylammonium and zinc ion on the resting conductance of frog skeletal muscle. *J. Physiol.* **209**, 231–256.

STANFIELD, P. R. (1977). A calcium dependent inward current in frog skeletal muscle fibres. *Pflügers Arch.* **368**, 267–270.

TASAKI, I., POLLEY, E. H. & ORREGO, F. (1954). Action potentials from individual elements in cat geniculate and striate cortex. *J. Neurophysiol.* **17**, 454–474.

ULBRICHT, W. & WÄGNER, H. H. (1975). The influence of pH on equilibrium effects of tetrodotoxin on myelinated nerve fibres of *Rana esculenta*. *J. Physiol.* **252**, 159–184.

VALDIOSERA, R., CLAUSEN, C. & EISENBERG, R. S. (1974). Measurement of the impedance of frog skeletal muscle fibers. *Biophys. J.* **14**, 295–315.

WARNER, A. E. (1972). Kinetic properties of the chloride conductance of frog muscle. *J. Physiol.* **227**, 291–312.

WEAST, R. C. & SELBY, S. M. (eds.). (1962). *Handbook of Chemistry and Physics*, 48th edn. Cleveland: Chemical Rubber Publishing Co.

WINEGRAD, S. (1968). Intracellular calcium movements of frog skeletal muscle during recovery from tetanus. *J. gen. Physiol.* **51**, 55–83.

YEH, J. Z., OXFORD, G. S., WU, C. H. & NARAHASHI, T. (1976). Dynamics of aminopyridine block of potassium channels in squid axon membrane. *J. gen. Physiol.* **68**, 519–535.